iScience

CellPress
OPEN ACCESS

Article

# Ing4-deficiency promotes a quiescent yet transcriptionally poised state in hematopoietic stem cells

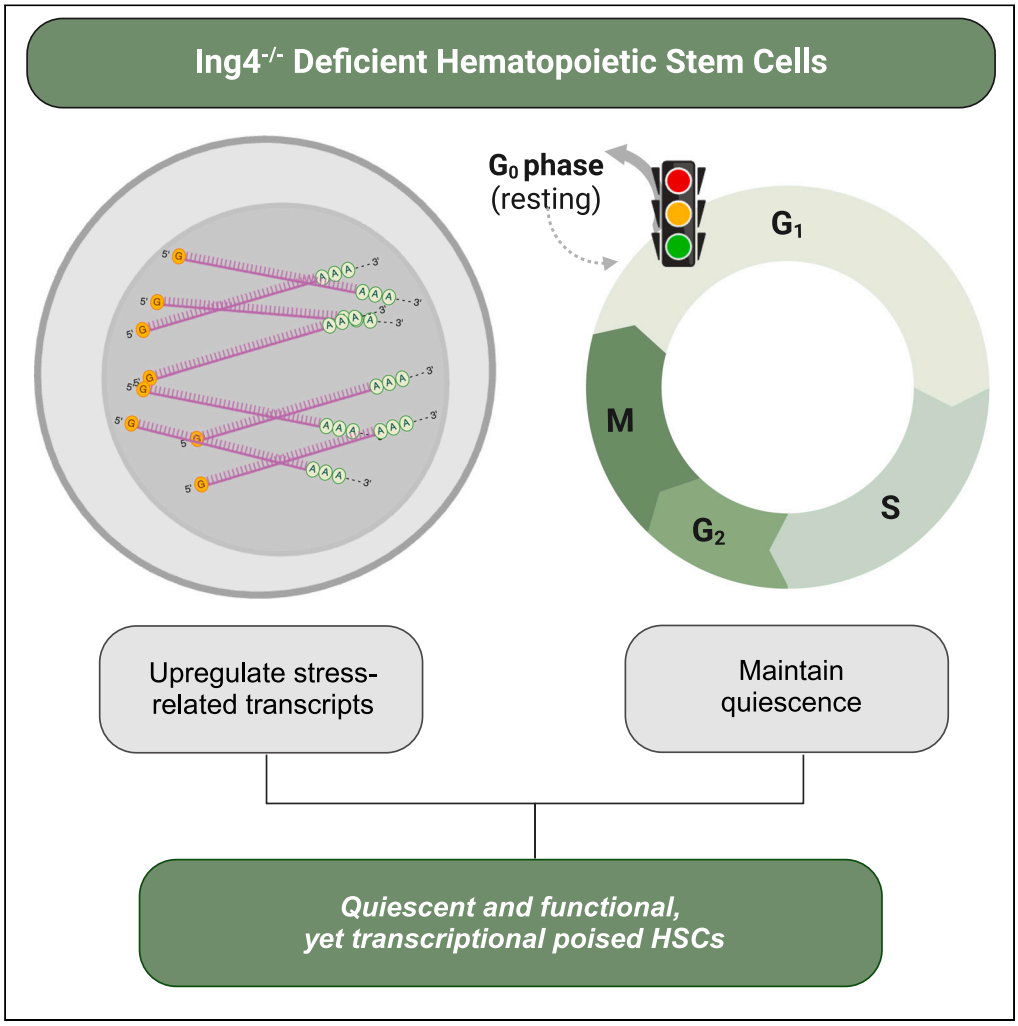


Zanshé Thompson, Georgina A. Anderson, Marco Hernandez, ..., Vera Binder, Alison M. Taylor, Katie L. Kathrein

klk@sc.edu

## Highlights

Loss of Ing4 promotes a poised state in hematopoietic stem cells (HSCs)

Ing4$^{-/-}$ HSCs have a transcriptional profile that reflects an activated, stressed HSC

Despite this, Ing4$^{-/-}$ HSCs are quiescent and functional in transplantation

Reducing c-Myc activity stimulates Ing4$^{-/-}$ HSCs into cycling

Thompson et al., iScience 27, 110521
August 16, 2024 
https://doi.org/10.1016/j.isci.2024.110521

iScience

CellPress
OPEN ACCESS

Article

# Ing4-deficiency promotes a quiescent yet transcriptionally poised state in hematopoietic stem cells

Zanshé Thompson,[1,5] Georgina A. Anderson,[2,5] Marco Hernandez,[2] Carlos Alfaro Quinde,[2] Alissa Marchione,[2] Melanie Rodriguez,[2] Seth Gabriel,[2] Vera Binder,[3] Alison M. Taylor,[4] and Katie L. Kathrein[2,6,*]

## SUMMARY

**Defining the mechanisms that regulate stem cell maintenance, proliferation, and differentiation is critical for identifying therapies for improving stem cell function under stress. Here, we have identified the tumor suppressor, inhibitor of growth 4 (Ing4), as a critical regulator of hematopoietic stem cell (HSC) homeostasis. Cancer cell line models with Ing4 deficiency have shown that Ing4 functions as a tumor suppressor, in part, due to Ing4-mediated regulation of several major signaling pathways, including c-Myc. In HSCs, we show Ing4 deficiency promotes gene expression signatures associated with activation, yet HSCs are arrested in $G_0$, expressing several markers of quiescence. Functionally, Ing4-deficient HSCs demonstrate robust regenerative capacity following transplantation. Our findings suggest Ing4 deficiency promotes a poised state in HSCs, where they appear transcriptionally primed for activation but remain in a resting state. Our model provides key tools for further identification and characterization of pathways that control quiescence and self-renewal in HSCs.**

## INTRODUCTION

Hematopoiesis is the process by which hematopoietic stem cells (HSCs) give rise to all mature blood cells.[1] HSCs simultaneously maintain quiescence and promote activation through tightly regulated cell-extrinsic and cell-intrinsic frameworks of proteins that maintain, promote, and repress specific gene expression patterns to enable production of blood for the lifespan of an organism.[2–7] This delicate balance allows for maintenance of a constant source for immune cell production while retaining a robust stem cell pool.[8–16] Disruption of the signaling pathways that maintain the stem cell pool can have significant consequences on the responsiveness, longevity, and strength of the immune system, often resulting in HSC exhaustion through chronic activation.[17–20] The importance of understanding hematopoiesis is clinically relevant, as hematopoietic stem exhaustion can result in bone marrow failure diseases, such as anemia, β-thalassemia, and inherited metabolic disorders.[21]

To uncover critical regulators of HSCs, we recently identified inhibitor of growth 4 (Ing4) in a zebrafish reverse genetic screen.[13] Ing4 is a tumor suppressor protein, generally localized to the nucleus, which is associated with a high frequency of acquired, inactivating mutations and poor prognoses in diverse human cancers.[22–26] Ing4 has many regulatory roles, both as a chromatin remodeling protein within the Hbo1 complex and as a direct regulator of several major signaling pathways: nuclear factor κB (NF-κB), c-Myc, p53, and HIF-1α.[27–32]

Previous work using a mouse model of Ing4 deficiency showed that $Ing4^{-/-}$ macrophages and neutrophils have increased NF-κB target gene expression and enhanced cytokine production upon exposure to lipopolysaccharides, suggesting a role for Ing4 in regulating differentiated immune cell responses.[32] Ing4 binds to the p65/RelA subunit of NF-κB, preventing p65 from binding to DNA, resulting in suppression of NF-κB target genes and inflammatory pathways.[29–31,33] In cancer cell line models, Ing4 has also been shown to interact directly with the c-Myc inhibitor, AUF1, to disrupt c-Myc function,[34] and the HIF-1α inhibitor, HPH-2, to disrupt HIF-1α function.[35] In addition, Ing4 enhances p53 function through acetylation.[36] These studies suggest that Ing4 is a critical regulatory protein, yet its role in hematopoiesis remains uncharacterized.

In this study, we identified an unexpected role for Ing4 as a negative regulator of HSC quiescence and self-renewal. Using an Ing4-deficient mouse model,[32] we show that Ing4 deficiency disrupts normal HSC populations. $Ing4^{-/-}$ HSCs display increased quiescence and they maintain low reactive oxygen species (ROS) levels and mitochondrial potential. Strikingly, loss of Ing4 expression has dueling outcomes for

[1]University of South Carolina, Department of Biomedical Engineering, Columbia, SC, USA
[2]University of South Carolina, Department of Biological Sciences, Columbia, SC, USA
[3]Department of Hematology and Oncology, Dr. von Hauner Children's Hospital, Ludwig-Maximilians University, 80539 Munich, Germany
[4]Columbia University Medical Center, Department of Pathology and Cell Biology, Herbert Irving Comprehensive Cancer Center, New York, NY 10032, USA
[5]These authors contributed equally
[6]Lead contact
*Correspondence: klk@sc.edu
https://doi.org/10.1016/j.isci.2024.110521

**Table 1. Cell types and corresponding surface markers used for identification**

| Cell Type | Surface Markers |
|---|---|
| LSK | $Lin^-$ $Sca\text{-}1^+$ $c\text{-}Kit^+$ |
| LT-HSC | $Lin^-$ $Sca\text{-}1^+$ $c\text{-}Kit^+$ $CD150^+$ $CD34^-$ |
| ST-HSC | $Lin^-$ $Sca\text{-}1^+$ $c\text{-}Kit^+$ $CD150^+$ $CD34^+$ |
| CLP | $Lin^-$ $Sca\text{-}1^{low}$ $c\text{-}Kit^{low}$ $CD127^+$ |
| MEP | $Lin^-$ $Sca\text{-}1^+$ $c\text{-}Kit^+$ $CD16/32^-$ $CD34^-$ |
| CMP | $Lin^-$ $Sca\text{-}1^+$ $c\text{-}Kit^+$ $CD16/32^-$ $CD34^+$ |
| GMP | $Lin^-$ $Sca\text{-}1^+$ $c\text{-}Kit^+$ $CD16/32^+$ $CD34^+$ |
| T cell | $CD3e^+$ |
| B cell | $B220^+$ |
| Macrophage | $Mac11b^+$ |
| Granulocyte | $Gr\text{-}1^+$ |
| RBC | $Ter119^+$ |

HSCs; they become more quiescent while simultaneously upregulating pathways associated with activation, creating a poised state. The quiescent state can be overcome though inhibition of c-Myc activity, which induces $Ing4^{-/-}$ HSCs into cycling. Our findings display an essential role for Ing4 in stem cell maintenance and activation.

## RESULTS

### The hematopoietic program is disrupted in the absence of Ing4

To investigate the role of Ing4 in hematopoiesis, we used a previously described Ing4-deficent mouse model to profile hematopoietic stem cells in the absence of Ing4 (Table 1).[32] Ing4 is highly expressed in murine HSCs, suggesting it may have a specific role in HSC function (see Figure S1A).[37,38] When compared with wild-type (WT) mice, there was no significant difference observed in the percentage and absolute number of $CD48^-$ $Lin^-Sca1^+c\text{-}Kit^+$ cells (LSKs) observed in the whole bone marrow (WBM) of $Ing4^{-/-}$ mice (see Figures S1B and S1C). Total nucleated cell numbers were similar for WT and $Ing4^{-/-}$ bone marrow (see Figure S1D). Recent publications have identified two distinct populations of HSCs: quiescent, repopulating long-term HSCs (LT-HSCs), and more actively dividing short-term HSCs (also termed $HSC^{ST}$, MPP1, and ST-HSCs; here designated ST-HSC)[4,39–45] (Gating strategy in Figure 1A). Analysis of these specific HSC populations showed that, in $Ing4^{-/-}$ mice, percentages and total numbers of LT-HSCs (LSK $CD48^-CD34^-CD150^+$) (Figures 1B and 1C) and ST-HSCs (LSK $CD48^-CD34^+CD150^+$) (Figures 1D and 1E) were significantly increased. These results suggest Ing4 deficiency may result in a differentiation block or expansion in HSCs.

Analysis of lineage committed cells in the WBM revealed no significant differences in progenitor populations or lineage positive ($Lin^+$) cell populations in the WBM of $Ing4^{-/-}$ mice (Gating Strategy in Figure 1F, population percentages shown in Figures 1G–1J, cell counts shown in Figures S1G–S1J). Thus, Ing4 is largely dispensable for maintenance of the committed progenitor pool.

### Ing4-deficient HSCs are quiescent and have low intracellular levels of reactive oxygen species and mitochondrial potential

We next investigated the cell-cycle status of $Ing4^{-/-}$ HSCs. The balance of quiescence and proliferation is essential for maintaining HSC populations.[46] Cell-cycle status of HSCs was analyzed using DAPI for DNA content and Ki-67 for proliferative status. Surprisingly, we found an increased proportion of cells in $G_0$ in both LT- and ST-HSC populations from $Ing4^{-/-}$ mice (Figures 2A–2D). To further interrogate if the increased proportions of cells in $G_0$ in LT- and ST-HSCs result from senescence in these populations or a phenotypic difference between the WT and $Ing4^{-/-}$ populations, we analyzed senescence-associated β-galactosidase (SA-β-gal) staining in WT and Ing4-deficient HSCs. We found slight increases in SA-β-gal activity in $Ing4^{-/-}$ LT- and ST-HSCs populations, but these differences were not statistically significant (Figures 2E–2I), suggesting that Ing4 deficiency likely does not trigger senescence in the majority of quiescent cells at this time point. As cell size correlates with quiescence, we also analyzed the forward scatter profiles of HSCs. $Ing4^{-/-}$ LT-HSCs are slightly smaller than WT LT-HSCs, though no significant difference in cell size was observed between WT and $Ing4^{-/-}$ ST-HSCs (see Figures S1E and S1F). These results further characterize the quiescent nature of $Ing4^{-/-}$ HSCs.

Ing4 has been shown to promote apoptosis through a direct interaction with p53.[47] Absence of Ing4 gives a competitive advantage to tumor cells by limiting p53 activity and, therefore, apoptosis. We therefore conducted assays with WT and $Ing4^{-/-}$ HSCs to determine if loss of Ing4 decreases apoptosis in these populations. When compared with WT HSCs, there was no significant difference in the frequency of cells undergoing apoptosis (annexin $V^+$) in the $Ing4^{-/-}$ HSC populations (see Figures S2D and S2E).

Previous studies show a direct link between HSC quiescence and low levels of intracellular ROS content.[48,49] To determine whether ROS levels are altered in $Ing4^{-/-}$ HSCs, we treated freshly isolated lineage depleted cells with 2′,7′-dichlorofluorescein diacetate ($H_2$DCFDA).

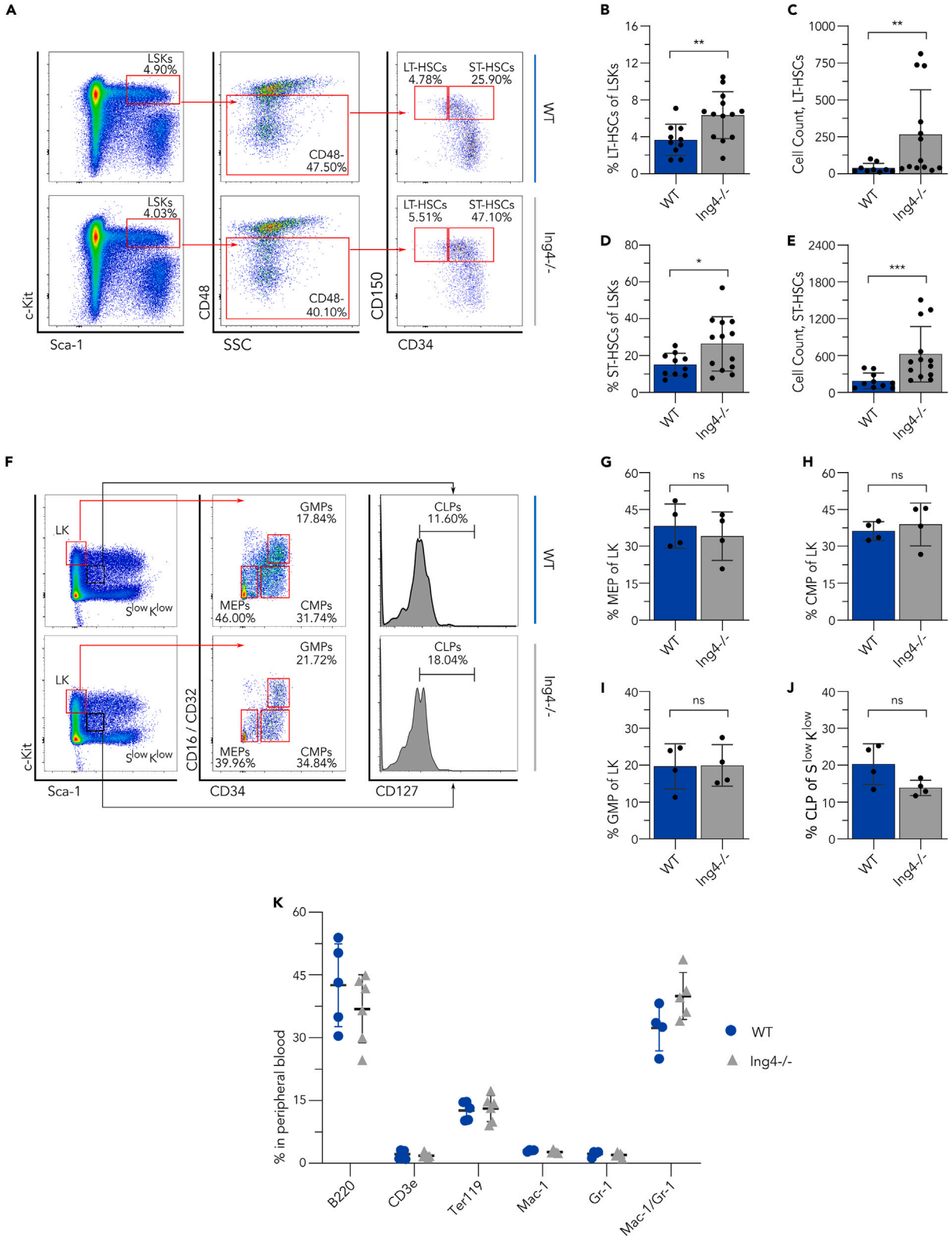
A
LSKs
4.90%
CD48-
47.50%
LT-HSCs
4.78%
ST-HSCs
25.90%
WT
LSKs
4.03%
CD48-
40.10%
LT-HSCs
5.51%
ST-HSCs
47.10%
Ing4-/-
c-Kit
Sca-1
CD48
SSC
CD150
CD34
B
% LT-HSCs of LSKs
C
Cell Count, LT-HSCs
D
% ST-HSCs of LSKs
E
Cell Count, ST-HSCs
WT
Ing4-/-
F
LK
GMPs
17.84%
MEPs
46.00%
CMPs
31.74%
CLPs
11.60%
GMPs
21.72%
MEPs
39.96%
CMPs
34.84%
CLPs
18.04%
CD16 / CD32
CD127
G
% MEP of LK
H
% CMP of LK
I
% GMP of LK
J
% CLP of S low K low
ns
K
% in peripheral blood
B220
CD3e
Ter119
Mac-1
Gr-1
Mac-1/Gr-1

**Figure 1. Deletion of Ing4 leads to skewed hematopoiesis in the bone marrow**

(A) Representative gating strategy of flow cytometric analysis for LT-HSCs and ST-HSCs.

(B) LT-HSCs from WBM isolated from individual WT and Ing4$^{-/-}$ steady state mice as a percentage of LSK cells. ($n$ = 10–13; **$p < 0.01$).

(C) Cell counts of LT-HSCs from WBM isolated from individual WT and Ing4$^{-/-}$ steady-state mice. ($n$ = 10–13; **$p < 0.01$).

(D) ST-HSCs from WBM isolated from individual WT and Ing4$^{-/-}$ steady state mice as a percentage of LSK cells. ($n$ = 10–13; *$p < 0.05$).

(E) Cell counts of ST-HSCs from WBM isolated from individual WT and Ing4$^{-/-}$ steady-state mice. ($n$ = 10–13; ***$p < 0.005$).

(F) Representative flow cytometric analysis of megakaryocyte-erythroid progenitors (MEP), common myeloid progenitor (CMP), granulocyte-macrophage progenitor (GMP), and common lymphoid progenitor (CLP) cell populations in WBM of WT and Ing4$^{-/-}$ steady-state mice.

(G) Percentages of lineage committed cell populations in the peripheral blood of WT and Ing4$^{-/-}$ steady-state mice as analyzed via flow cytometry. ($n$ = 5–6; ns = $p > 0.05$).

(H) MEP from WBM isolated from individual WT and Ing4$^{-/-}$ steady-state mice as a percentage of LK cells. ($n$ = 4; ns = $p > 0.05$).

(I) CMP from WBM isolated from individual WT and Ing4$^{-/-}$ steady-state mice as a percentage of LK cells. ($n$ = 4; ns = $p > 0.05$).

(J) GMP from WBM isolated from individual WT and Ing4$^{-/-}$ steady-state mice as a percentage of LK cells. ($n$ = 4; ns = $p > 0.05$).

(K) CLP from WBM isolated from individual WT and Ing4$^{-/-}$ steady-state mice as a percentage of $S^{low}K^{low}$ cells. ($n$ = 4; ns = $p > 0.05$).

Data in (B), (D), (H), (I), (J), and (K) reflect mean values ± SD. Statistical significance was assessed using Student's t test with Welch's correction. Data in (C) and (E) reflect mean values ± SD. Statistical significance was assessed using Mann-Whitney analysis.

Ing4$^{-/-}$ LT- and ST-HSCs trend toward lower, but not significantly different, levels of ROS content compared to WT controls (Figures 3A–3E). These results correlate with Ing4$^{-/-}$ HSC quiescence levels.

Finally, to investigate metabolic activation, we looked at tetramethylrhodamine methyl ester (TMRM) levels for the detection of mitochondrial membrane potential state as a marker for cell activation. Upon activation, HSCs undergo a switch from glycolysis to oxidative phosphorylation (OXPHOS) to generate ATP, creating electrical potential difference across the mitochondrial membrane that results in TMRM staining.[50,51] Comparing WT and Ing4$^{-/-}$ HSCs, we observe similar TMRM levels, suggesting that Ing4$^{-/-}$ HSCs have similar membrane potential to WT, denoting similar OXPHOS usage as an energy source to WT HSCs (Figures 3F–3J). Taken together with our findings of cell cycle and ROS profiling of Ing4$^{-/-}$ HSCs, these data provide evidence that Ing4$^{-/-}$ HSCs persist in a sustained resting state.

## Ing4$^{-/-}$ HSCs simultaneously express genes associated with activation and quiescence

To elucidate the molecular consequences of Ing4 loss in HSC regulation, we conducted a genome-wide expression analysis using bulk RNA-sequencing (RNA-seq) of purified Ing4$^{-/-}$ LT-HSCs and ST-HSCs and compared the profiles of these populations, pooled, against pooled wild-type LT-HSC and ST-HSC gene expression. This analysis revealed 2,420 differentially expressed genes in the combined populations (1,139 upregulated and 1,281 downregulated, $p < 0.05$) (Figures 4A and 4B). Surprisingly, gene set enrichment analysis (GSEA) of this dataset using the gene ontology biological process (GOBP) gene set showed upregulated genes in Ing4$^{-/-}$ HSCs that were associated with oxidative phosphorylation, ribosomal biogenesis, and c-Myc target gene expression. Downregulated genes were associated with mitotic spindle formation and cytoskeletal modification (Figure 4A). All dysregulated genes are represented in a volcano plot shown in Figure 4B. The 100 genes with greatest magnitude of up- or downregulation are shown in Figures S3A and S3B. Several genes upregulated in RNA-seq were validated with qPCR (Figures 4C–4F). Results from qPCR analysis show a statistically significant positive correlation with RNA-seq data (Figure 4C). These data are also shown as individual genes, with relative fold changes analyzed by qPCR and compared to housekeeping gene expression (Figures 4D and 4F). A set of genes that are associated with HSC quiescence and cell cycle regulation were also upregulated, including the cell-cycle regulator p57 in both the RNA-seq data (Figure 4B) and by qPCR (Figure 4F). Together, these signatures suggest that Ing4 deficiency may promote a transcriptionally poised state in HSCs, whereby Ing4 loss upregulates genes associated with activation while also inducing quiescence-associated genes to maintain HSCs in a resting state.

## Ing4-deficient HSCs demonstrate normal responses in stress hematopoiesis

To analyze the functional role of Ing4 deficiency in HSC reconstitution, we competitively transplanted WBM cells from Ing4$^{-/-}$ and WT mice into lethally (9.5Gy) irradiated WT recipients (1:4 ratio) (Figures 5A and 5B). Peripheral blood analysis at 4- and 12-week post-transplantation showed no significant difference in donor contribution of Ing4$^{-/-}$ cells in comparison to WT cells (Figures 5C and 5D) nor was there significantly altered lineage distribution observed (Figures 5E–5G). This suggests that Ing4-deficient bone marrow is capable of engraftment at wild-type levels.

To compare the reconstitution and maintenance capacity of Ing4-deficient HSC subsets, we transplanted sorted LT-HSCs and ST-HSCs from CD45.2 Ing4$^{-/-}$ and WT mice in a competitive setting. To this end, we transplanted either 10 LT-HSCs or 50 ST-HSCs combined with 200,000 CD45.1 unfractionated WBM cells. PB analysis at 4-, and 12-week post-transplantation revealed a significant absence of donor contribution in the Ing4$^{-/-}$ LT-HSCs in comparison to WT LT-HSC, though chimerism is very low for both groups (see Figure S4). There were no significant differences in the chimerism observed in transplanted ST-HSC populations (Figure 4G). These results suggest Ing4$^{-/-}$ LT-HSCs may be incapable of repopulation, whereas ST-HSCs have robust repopulating activity.

To examine if proliferation may be impaired in the absence of Ing4 and contributing to loss of LT-HSC function in transplantation, we performed an *in vitro* cell proliferation assay. WBM was harvested, stained with cell trace violet (CTV), and cultured for 7 days. Ing4$^{-/-}$ ST-HSCs proliferate at similar rates to WT ST-HSCs, but Ing4$^{-/-}$ LT-HSCs are less proliferative than their WT counterparts, with more cells that have not undergone cell division by 7 days (Figures 5H–5J).

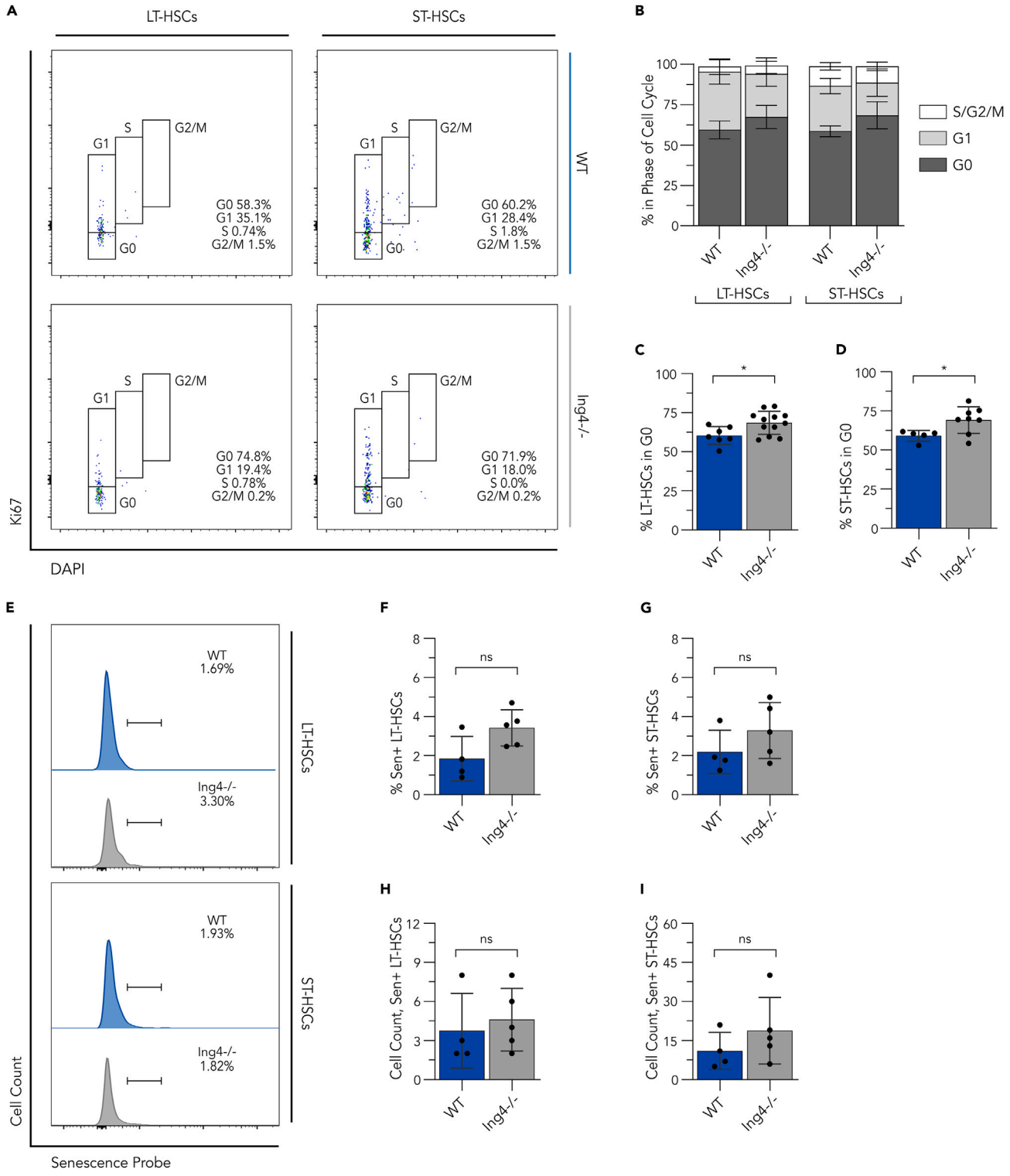


**Figure 2. Ing4-deficient HSCs have increased quiescence**

(A) Representative flow cytometric analysis of LT-HSCs and ST-HSCs using Ki-67 and DAPI for cell cycle profile.

(B) Mean values and standard deviations of all cell-cycle phases for LT-HSC and ST-HSC populations in WT and Ing4$^{-/-}$ bone marrow at steady state.

(C) LT-HSCs in $G_0$ isolated from bone marrow of individual WT and Ing4$^{-/-}$ steady-state mice as a percentage of the LT-HSC population. ($n$ = 5–9; * = $p < 0.05$).

(D) ST-HSCs in $G_0$ isolated from bone marrow of individual WT and Ing4$^{-/-}$ steady-state mice as a percentage of the ST-HSC population. ($n$ = 5–9; * = $p < 0.05$).

**Figure 2. *Continued***

(E) Representative flow cytometric analysis of β-galactosidase staining for senescence in LT-HSC and ST-HSC populations in WT and Ing4$^{-/-}$ bone marrow at steady state. Figure S2A shows negative and positive histogram profiles for senescence.

(F) Senescence-positive LT-HSCs isolated individual WT and Ing4$^{-/-}$ steady-state mice as a percentage of all LT-HSCs. ($n$ = 4–5; ns = $p > 0.05$).

(G) Senescence-positive ST-HSCs isolated from individual WT and Ing4$^{-/-}$ steady-state mice as a percentage of all ST-HSCs. ($n$ = 4–5; ns = $p > 0.05$).

(H) Cell counts of senescence-positive LT-HSCs from WBM isolated from individual WT and Ing4$^{-/-}$ steady-state mice. ($n$ = 4–5; ns = $p > 0.05$).

(I) Cell counts of senescence-positive ST-HSCs from WBM isolated from individual WT and Ing4$^{-/-}$ steady-state mice. ($n$ = 4–5; ns = $p > 0.05$).

Data in (C), (D), (F), (G), and (I) reflect mean values ± SD. Statistical significance was assessed using Student's t test with Welch's correction. Data in (H) reflect mean values ± SD. Statistical significance was assessed using Mann-Whitney analysis.

To further dissect hematopoietic function in the absence of Ing4, we studied the response of Ing4$^{-/-}$ HSCs to hematopoietic stress induced by the myeloablative agent 5-fluorouracil (5-FU) as a mechanism to trigger HSC activation (Figure 6A). Following single dose 5-FU- or mock-treatment, there was no significant difference in Ing4$^{-/-}$ LT-HSCs populations in the bone marrow at 15 days (Figures 6B and 6C). In contrast, bone marrow from WT mice treated with 5-FU exhibited a significant increase in LT-HSCs as a proportion of LSKs at 15 days post-treatment compared to mice receiving mock treatment (Figure 6B). This suggests that Ing4$^{-/-}$ LT-HSCs are not responding to 5-FU treatment.

We found Ing4$^{-/-}$ ST-HSCs to be significantly decreased in mice treated with 5-FU as compared to those receiving mock treatment at 15 days post-injection, while at the same time point, there was no significant difference between ST-HSCs of WT mice who received 5-FU or mock (Figures 6D and 6E). These data indicate that 5-FU ablation may remove a differentiation block or trigger apoptosis in Ing4$^{-/-}$ ST-HSCs at 15 days post-5-FU or -mock treatment.

By 30 days post-treatment, no significant differences between Ing4$^{-/-}$ HSCs were observed in mice who received 5-FU or mock treatment (Figures 6F–6I) by percent of LSK. We noted lower trending LT- and ST-HSCs in the bone marrow of Ing4$^{-/-}$ mice treated with 5-FU than WT mice receiving 5-FU injections at 30 days post-treatment (Figures 6F–6I), but this is only significant by cell count in ST-HSCs. These results suggest Ing4$^{-/-}$ HSCs ultimately respond to ablation and return to near pretreatment levels, albeit the response is delayed compared to WT HSCs.

## c-Myc inhibitor enhances HSC recovery

We also used sublethal (3.5Gy), low-dose irradiation (LDI) as an alternative insult to target dividing cells (Figure 7A). 14 days post-irradiation, Ing4$^{-/-}$ LT- and ST-HSCs showed significantly more cells in $G_0$ compared to WT LT- and ST-HSCs, suggesting a diminished or delayed response to LDI in Ing4$^{-/-}$ HSCs (Figures 7B and 7E).

Next, we sought to determine if targeted chemical perturbation of Ing4$^{-/-}$ HSCs could impact the quiescent state of Ing4$^{-/-}$ HSCs. We focused on the c-Myc pathway for several reasons: (1) c-Myc target genes are over-represented in our RNA-seq data, (2) c-Myc lies upstream of several of the other mis-regulated pathways observed in Ing4$^{-/-}$ HSCs, and (3) Ing4 was previously reported to negatively regulate c-Myc target gene expression.[34,52] Recognizing the myriad impact of the c-Myc pathway, we hypothesized that by targeting c-Myc activity, we could trigger a dampening of many of the upregulated genes in Ing4$^{-/-}$ HSCs through diminishing c-Myc target gene expression, thus achieving a level of c-Myc target gene expression closer to WT levels. Considering our observation of increased quiescence in Ing4$^{-/-}$ HSCs, we conducted an *in vivo* assay whereby WT and Ing4$^{-/-}$ mice were treated with a c-Myc dimerization inhibitor, 10058-F4, following hematopoietic insult by sublethal irradiation. This allowed us to ascertain whether Ing4$^{-/-}$ HSC quiescence could be relieved through inhibition of c-Myc activity.[53,54] We found that, in Ing4$^{-/-}$ mice, the inhibitor stimulated both LT-HSCs and ST-HSCs to begin cycling (Figures 7B–7G). Cell-cycle analysis of c-Myc inhibitor-treated HSCs revealed decreased percentages of Ing4$^{-/-}$ LT- and ST-HSCs in the $G_0$ phase of the cell cycle compared to untreated Ing4$^{-/-}$ HSCs (Figures 7C and 7F). These data demonstrate inhibition of c-Myc activity releases Ing4$^{-/-}$ HSCs from $G_0$ arrest, allowing them to proceed through the cell cycle.

## DISCUSSION

The exact molecular mechanisms that allow for the maintenance of HSC homeostasis in the bone marrow, including quiescence, self-renewal, and activation, remain elusive. In this study, we describe a role for Ing4 in regulation of HSC homeostasis. Prior to our work, no role for Ing4 had been identified in murine hematopoiesis. Here, we show that Ing4 plays a critical role as a vital regulator of HSC maintenance and self-renewal in several key ways: (1) Ing4 deficiency induces a poised state in HSCs, where HSCs are quiescent, yet transcriptionally primed for activation, (2) Ing4-deficient HSCs are functional, with the ability to repopulate the bone marrow in transplantation assays and recover from 5-FU treatment or LDI, and (3) modulation of c-Myc activity can mitigate the cell-cycle arrest in Ing4-deficient HSCs.

Ing4 deficiency results in skewed hematopoiesis, with a subtle increase in LT-HSCs, and a more marked increase in ST-HSCs. Both LT-HSCs and ST-HSCs are more quiescent than their wild-type counterparts. Transcriptional profiling of Ing4$^{-/-}$ HSCs show that they more closely resemble activated cells or more differentiated hematopoietic progenitors rather than quiescent HSCs. Specifically, markers of oxidative phosphorylation, ribosomal biogenesis, and other c-Myc target genes are significantly upregulated in Ing4$^{-/-}$ HSCs, more closely matching profiles of differentiating HSCs or progenitors.[55–59] Surprisingly, examination of the levels of ROS, mitochondrial potential, and cell size in Ing4$^{-/-}$ HSCs showed no differences from wild type. These data, coupled with the quiescent status of the Ing4$^{-/-}$ HSCs, suggest that although we observe transcriptional upregulation of activation-associated genes, the resting, quiescent state of the HSCs may prevent the conversion from this poised state to an active state.

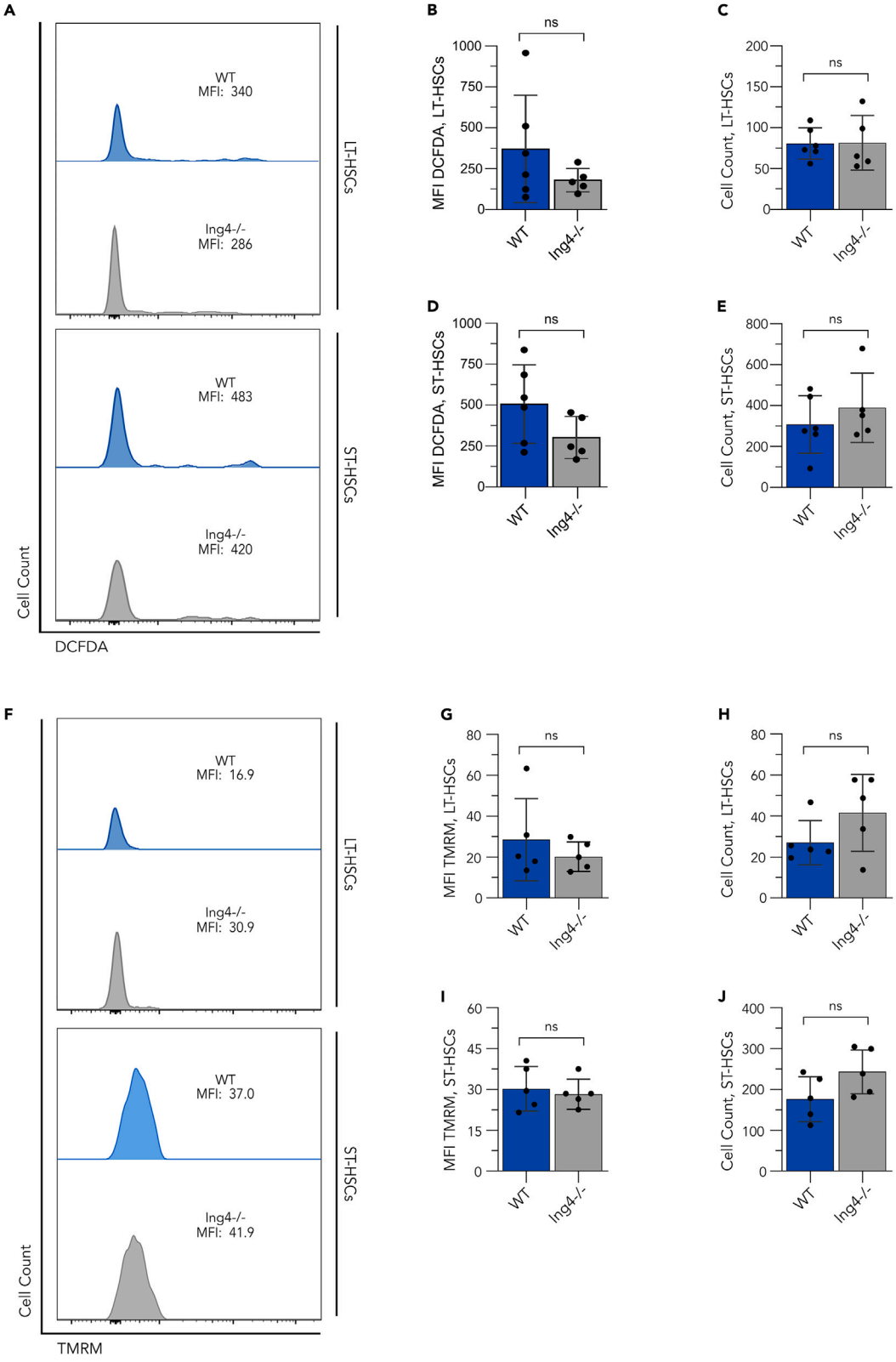
A
WT
MFI: 340
Ing4-/-
MFI: 286
LT-HSCs
WT
MFI: 483
Ing4-/-
MFI: 420
ST-HSCs
Cell Count
DCFDA
B
MFI DCFDA, LT-HSCs
ns
C
Cell Count, LT-HSCs
ns
D
MFI DCFDA, ST-HSCs
ns
E
Cell Count, ST-HSCs
ns
F
WT
MFI: 16.9
Ing4-/-
MFI: 30.9
LT-HSCs
WT
MFI: 37.0
Ing4-/-
MFI: 41.9
ST-HSCs
Cell Count
TMRM
G
MFI TMRM, LT-HSCs
ns
H
Cell Count, LT-HSCs
ns
I
MFI TMRM, ST-HSCs
ns
J
Cell Count, ST-HSCs
ns
WT
Ing4-/-

**Figure 3. Ing4-deficient HSCs have low levels of reactive oxygen species and mitochondrial potential**

(A) Representative flow cytometric analysis of staining with DCFDA for ROS in LT-HSC and ST-HSC populations in WT and Ing4$^{-/-}$ bone marrow at steady state. Figure S2B shows negative and positive histogram profiles for ROS staining via flow cytometry.

(B) MFI of DCFDA in LT-HSCs isolated from individual WT and Ing4$^{-/-}$ steady-state mice. ($n$ = 5–6; ns = $p > 0.05$).

(C) Cell counts of LT-HSCs from WBM isolated from individual WT and Ing4$^{-/-}$ steady-state mice. ($n$ = 5–6; ns = $p > 0.05$).

(D) MFI of DCFDA in ST-HSCs isolated from individual WT and Ing4$^{-/-}$ steady-state mice. ($n$ = 5–6; ns = $p > 0.05$).

(E) Cell counts of ST-HSCs from WBM isolated from individual WT and Ing4$^{-/-}$ steady-state mice. ($n$ = 5–6; ns = $p > 0.05$).

(F) Representative flow cytometric analysis of staining for TMRM in LT-HSC and ST-HSC populations in WT and Ing4$^{-/-}$ bone marrow at steady state. Figure S2C shows negative, carbonyl cyanide m-chlorophenylhydrazone (CCCP) treated, and positive histogram profiles for TMRM staining via flow cytometry.

(G) MFI of TMRM-treated LT-HSCs isolated from individual WT and Ing4$^{-/-}$ steady-state mice. ($n$ = 5; ns = $p > 0.05$).

(H) Cell counts of LT-HSCs from WBM isolated from individual WT and Ing4$^{-/-}$ steady-state mice. ($n$ = 5; ns = $p > 0.05$).

(I) MFI of TMRM-treated ST-HSCs isolated from individual WT and Ing4$^{-/-}$ steady-state mice. ($n$ = 5; ns = $p > 0.05$).

(J) Cell counts of ST-HSCs from WBM isolated from individual WT and Ing4$^{-/-}$ steady-state mice. ($n$ = 5; ns = $p > 0.05$).

Data in (B), (C), (E), (G), (I), and (J) reflect mean values ± SD. Statistical significance was assessed using Student's t test with Welch's correction. Data in (D) and (H) reflect mean values ± SD. Statistical significance was assessed using Mann-Whitney analysis.

Enhanced or enforced HSC quiescence is a hallmark of a subset of dormant or latent hematopoietic stem cells.[60–62] Although the transcriptional profiles of latent HSCs vary from Ing4$^{-/-}$ HSCs, these studies suggest that Ing4$^{-/-}$ HSCs may retain functional latency despite their transcriptional profiles. Quiescence markers such as p57 are transcriptionally upregulated in Ing4$^{-/-}$ HSCs, providing a potential mechanism for latency maintenance.[7,63–70] Future studies will focus on whether Ing4 directly regulates these quiescence markers.

To overcome the enforced quiescence in Ing4$^{-/-}$ HSCs, we used LDI followed by treatment with a c-Myc inhibitor to potentially target several of the pathways transcriptionally overexpressed in our RNA-seq analysis, including ribosomal biogenesis, oxidative phosphorylation, and c-Myc target gene expression. This inhibitor triggered proliferation in both LT-HSCs and ST-HSCs. These results suggest that quiescence in Ing4-deficienct HSCs can be partially overcome through targeting of c-Myc activity.[71] Our data suggest that a relationship between Ing4 and c-Myc activity, either direct or indirect, may be the driving force behind the poised state we observe in Ing4-deficient HSCs, but the exact nature of this interaction remains to be determined. c-Myc has long been considered to play a vital role in cell cycle progression, and recent studies have added insight into the complexity of c-Myc function in hematopoiesis, more specifically as a mediator of stem cell quiescence and self-renewal.[72,73]

Mechanistically, c-Myc is believed to selectively activate transcription of genes encoding for oxidative phosphorylation (IDH3A, IDH3B, IDH3G, NDUFB7, SDHB, UQCR10, and COX5B) in p27$^{high}$Ki67$^{low}$ quiescent, rather than cycling, cells.[74] Notably, this is similar to results observed in our Ing4$^{-/-}$ LT- and ST-HSCs. Studies using melanoma and lung cancer cells have reported upregulated expression of both c-Myc and p27, which drive cancer cells into quiescence.[74] Loss of a single c-Myc allele resulted in decreased HSC quiescence and impaired repopulation capacity, further highlighting its necessity for HSC quiescence.[75] Yet, c-Myc inactivation can result in an accumulation of HSCs and diminished HSC function,[72,76] although an *in vitro* study has suggested that c-Myc loss enhances HSC expansion in culture.[77] Enforced expression of c-Myc results in HSC loss of function, at least in part through N-cadherin and integrin downregulation. These findings suggest that specific levels of c-Myc activity may dictate HSC function and could account for the disparate data in the literature, and may suggest a mechanism for Ing4$^{-/-}$ HSC deregulation. Future work will be focused on determining the exact mechanism for this phenotype, specifically if c-Myc activity is directly regulated by Ing4 and gives rise to the resulting c-Myc target gene expression, or if Ing4 functions downstream of c-Myc to regulate c-Myc target gene expression.

Our results demonstrate for the first time the importance of Ing4 regulation of several pathways required for hematopoiesis. Ing4 deficiency places hematopoietic stem cells in a peculiar state, with a transcriptional profile of activation, but without the normally observed functional HSC phenotypes typically associated with this profile, including the inability to contribute to chimerism during transplantation, skewed hematopoiesis, and exhaustion. Our results suggest a potential disconnect between transcription and production of functioning proteins in the absence of Ing4. However, normal HSCs have been shown to maintain high levels of ribosomal biogenesis during quiescence without translational changes, so Ing4$^{-/-}$ HSCs may utilize normal pathways to maintain further elevated levels of ribosomal components and other transcripts while maintaining normal levels of translation.[78,79] Alternatively, Ing4 has been linked to regulation of mRNA processing as a mechanism for regulation of c-Myc target gene expression.[34,80] Perhaps there is an expanded role for this pathway in the absence of Ing4 in hematopoietic stem cells. As well, expression of the mRNA m$^6$a reader, YTHDF2, is transcriptionally upregulated in Ing4$^{-/-}$ HSCs, providing a potential mechanism for mRNA decay, which might contribute to the observed disconnect between Ing4$^{-/-}$ HSCs transcriptional profile and functional outcomes.[55] Future work will focus on determining the exact mechanism for this phenotype.

## Limitations of the study

Many similarities are observed between the Ing4$^{-/-}$ LT- and ST-HSCs, but we do observe some differences that remain to be fully elucidated and represent a limitation of the scope of this study. Specifically, at 15 days post 5-FU treatment we observed differing effects on Ing4$^{-/-}$ ST-HSCs, with an observed a loss of ST-HSCs following 5-FU treatment that is not observed for LT-HSCs, which do not respond to 5-FU treatment. Both cell types return to mock treatment levels by 30 days by percent of LSK. We did observe a trend of lower LT- and ST-HSCs in the bone marrow of Ing4$^{-/-}$ mice treated with 5-FU than WT mice receiving 5-FU injections at 30 days post-treatment (Figures 6F–6I), but this is only significant by cell count in ST-HSCs and becomes less significant from 15 days to 30 days post-treatment. Further work will focus on if ST-HSCs are more sensitive to hematopoietic insults than their wild-type counterparts.

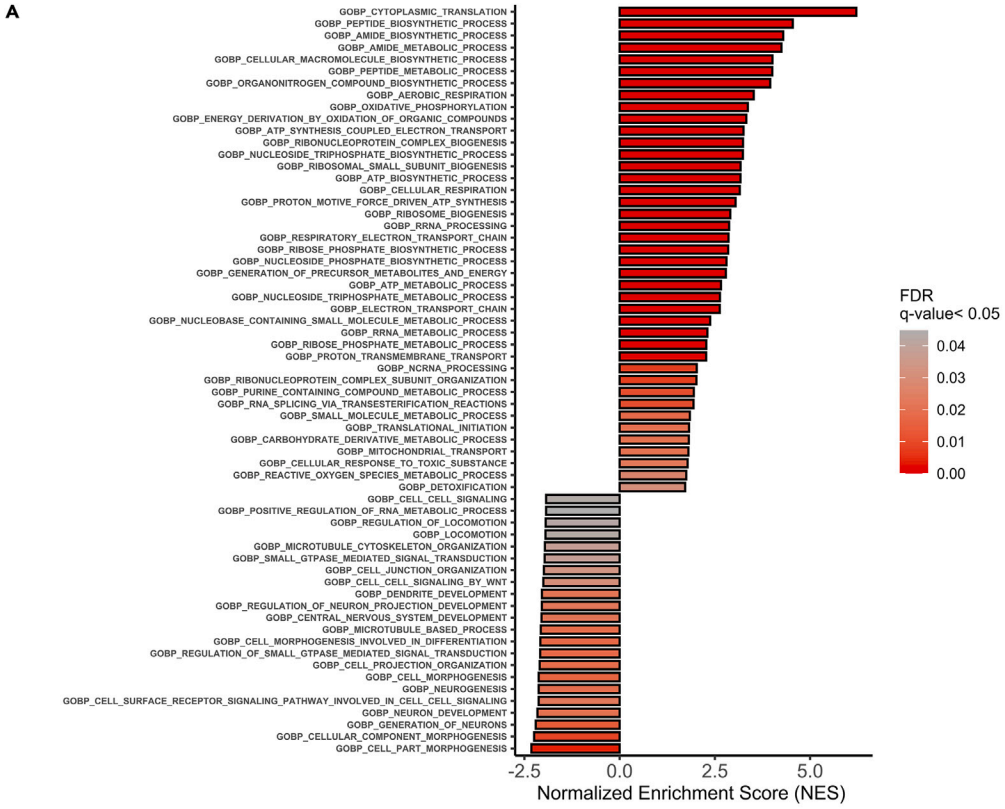
A
GOBP_CYTOPLASMIC_TRANSLATION
GOBP_PEPTIDE_BIOSYNTHETIC_PROCESS
GOBP_AMIDE_BIOSYNTHETIC_PROCESS
GOBP_AMIDE_METABOLIC_PROCESS
GOBP_CELLULAR_MACROMOLECULE_BIOSYNTHETIC_PROCESS
GOBP_PEPTIDE_METABOLIC_PROCESS
GOBP_ORGANONITROGEN_COMPOUND_BIOSYNTHETIC_PROCESS
GOBP_AEROBIC_RESPIRATION
GOBP_OXIDATIVE_PHOSPHORYLATION
GOBP_ENERGY_DERIVATION_BY_OXIDATION_OF_ORGANIC_COMPOUNDS
GOBP_ATP_SYNTHESIS_COUPLED_ELECTRON_TRANSPORT
GOBP_RIBONUCLEOPROTEIN_COMPLEX_BIOGENESIS
GOBP_NUCLEOSIDE_TRIPHOSPHATE_BIOSYNTHETIC_PROCESS
GOBP_RIBOSOMAL_SMALL_SUBUNIT_BIOGENESIS
GOBP_ATP_BIOSYNTHETIC_PROCESS
GOBP_CELLULAR_RESPIRATION
GOBP_PROTON_MOTIVE_FORCE_DRIVEN_ATP_SYNTHESIS
GOBP_RIBOSOME_BIOGENESIS
GOBP_RRNA_PROCESSING
GOBP_RESPIRATORY_ELECTRON_TRANSPORT_CHAIN
GOBP_RIBOSE_PHOSPHATE_BIOSYNTHETIC_PROCESS
GOBP_NUCLEOSIDE_PHOSPHATE_BIOSYNTHETIC_PROCESS
GOBP_GENERATION_OF_PRECURSOR_METABOLITES_AND_ENERGY
GOBP_ATP_METABOLIC_PROCESS
GOBP_NUCLEOSIDE_TRIPHOSPHATE_METABOLIC_PROCESS
GOBP_ELECTRON_TRANSPORT_CHAIN
GOBP_NUCLEOBASE_CONTAINING_SMALL_MOLECULE_METABOLIC_PROCESS
GOBP_RRNA_METABOLIC_PROCESS
GOBP_RIBOSE_PHOSPHATE_METABOLIC_PROCESS
GOBP_PROTON_TRANSMEMBRANE_TRANSPORT
GOBP_NCRNA_PROCESSING
GOBP_RIBONUCLEOPROTEIN_COMPLEX_SUBUNIT_ORGANIZATION
GOBP_PURINE_CONTAINING_COMPOUND_METABOLIC_PROCESS
GOBP_RNA_SPLICING_VIA_TRANSESTERIFICATION_REACTIONS
GOBP_SMALL_MOLECULE_METABOLIC_PROCESS
GOBP_TRANSLATIONAL_INITIATION
GOBP_CARBOHYDRATE_DERIVATIVE_METABOLIC_PROCESS
GOBP_MITOCHONDRIAL_TRANSPORT
GOBP_CELLULAR_RESPONSE_TO_TOXIC_SUBSTANCE
GOBP_REACTIVE_OXYGEN_SPECIES_METABOLIC_PROCESS
GOBP_DETOXIFICATION
GOBP_CELL_CELL_SIGNALING
GOBP_POSITIVE_REGULATION_OF_RNA_METABOLIC_PROCESS
GOBP_REGULATION_OF_LOCOMOTION
GOBP_LOCOMOTION
GOBP_MICROTUBULE_CYTOSKELETON_ORGANIZATION
GOBP_SMALL_GTPASE_MEDIATED_SIGNAL_TRANSDUCTION
GOBP_CELL_JUNCTION_ORGANIZATION
GOBP_CELL_CELL_SIGNALING_BY_WNT
GOBP_DENDRITE_DEVELOPMENT
GOBP_REGULATION_OF_NEURON_PROJECTION_DEVELOPMENT
GOBP_CENTRAL_NERVOUS_SYSTEM_DEVELOPMENT
GOBP_MICROTUBULE_BASED_PROCESS
GOBP_CELL_MORPHOGENESIS_INVOLVED_IN_DIFFERENTIATION
GOBP_REGULATION_OF_SMALL_GTPASE_MEDIATED_SIGNAL_TRANSDUCTION
GOBP_CELL_PROJECTION_ORGANIZATION
GOBP_CELL_MORPHOGENESIS
GOBP_NEUROGENESIS
GOBP_CELL_SURFACE_RECEPTOR_SIGNALING_PATHWAY_INVOLVED_IN_CELL_CELL_SIGNALING
GOBP_NEURON_DEVELOPMENT
GOBP_GENERATION_OF_NEURONS
GOBP_CELLULAR_COMPONENT_MORPHOGENESIS
GOBP_CELL_PART_MORPHOGENESIS
-2.5
0.0
2.5
5.0
Normalized Enrichment Score (NES)
FDR
q-value< 0.05
0.04
0.03
0.02
0.01
0.00

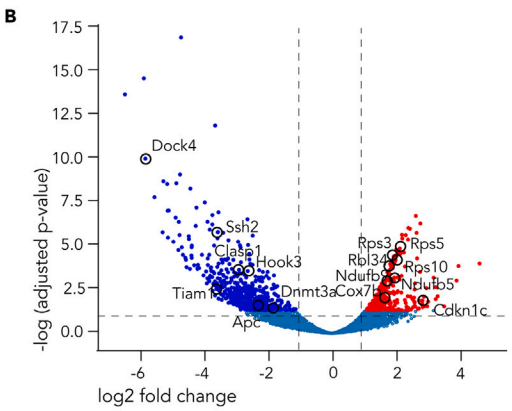
B
-log (adjusted p-value)
log2 fold change
Dock4
Ssh2
Clasp1
Hook3
Tiam1
Dnmt3a
Apc
Rps3
Rps5
Rpl34
Rps10
Ndufb5
Cox7b
Cdkn1c

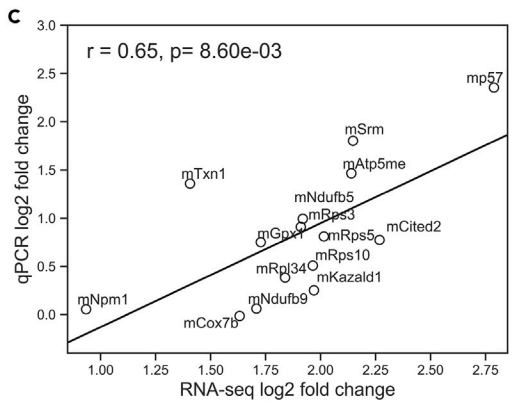
C
r = 0.65, p= 8.60e-03
qPCR log2 fold change
RNA-seq log2 fold change
mp57
mSrm
mAtp5me
mTxn1
mNdufb5
mRps3
mGpx1
mRps5
mCited2
mRps10
mRpl34
mKazald1
mNpm1
mNdufb9
mCox7b

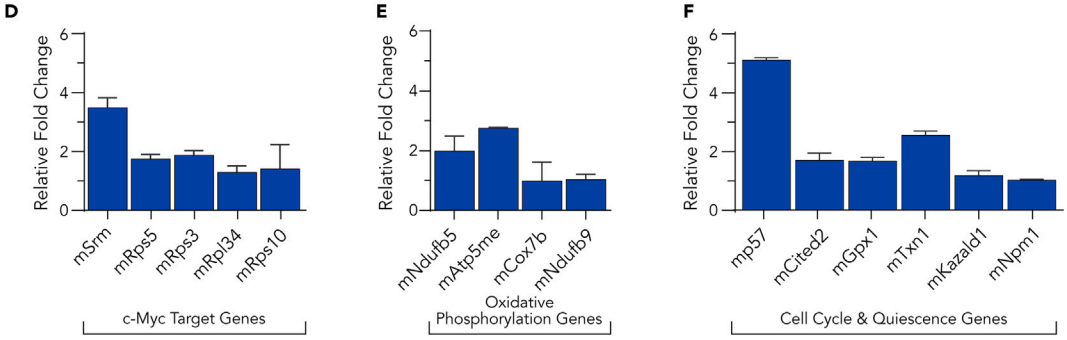
D
Relative Fold Change
mSrm
mRps5
mRps3
mRpl34
mRps10
c-Myc Target Genes
E
Relative Fold Change
mNdufb5
mAtp5me
mCox7b
mNdufb9
Oxidative Phosphorylation Genes
F
Relative Fold Change
mp57
mCited2
mGpx1
mTxn1
mKazald1
mNpm1
Cell Cycle & Quiescence Genes

**Figure 4. Gene expression analysis of Ing4$^{-/-}$ HSC populations**

(A) Normalized enrichment scores (NES) from a gene ontology biological process (GOBP) gene set analysis comparing two populations (WT LT- and ST-HSCs pooled), and (null LT- and ST-HSCs pooled). A total of 63 enrichment pathways (FDR-adjusted $p$ value<0.05) were identified. Bar colors indicate statistical significance.

(B) Differentially expressed genes in pooled WT LT-HSCs and ST-HSCs compared to pooled Ing4$^{-/-}$ LT-HSCs and ST-HSCs, with a statistically significant threshold of $p < 0.05$, and a $Log_2$Fold change = 1. Upregulated genes are represented in red, downregulated in blue. Highlighted genes in red are validated from qPCR data. Highlighted genes in blue are associated with the mitotic spindle formation.

(C) Positive correlation of RNA-sequencing expression data and qPCR expression data. Log2-fold change values were analyzed and plotted for 14 differentially expressed genes. The solid reference line represents the linear relationship.

(D) qPCR analysis of c-Myc target gene expression in cDNA generated from RNA collected from pooled LT- and ST-HSCs of WT or Ing4$^{-/-}$ WBM.

(E) qPCR analysis quantifying expression of genes associated with oxidative phosphorylation in cDNA generated from RNA collected from pooled LT- and ST-HSCs of WT or Ing4$^{-/-}$ WBM.

(F) qPCR analysis quantifying expression of genes associated with cell cycle regulation and quiescence in cDNA generated from RNA collected from pooled LT- and ST-HSCs of WT or Ing4$^{-/-}$ WBM.

We also observe a difference in contribution to chimerism in the sorted LT-HSC and ST-HSC transplantations. The chimerism in our LT-HSC transplantation assay is low and needs further exploration to make definitive conclusions, though the data suggest that loss of Ing4 impairs function of LT-HSCs but not ST-HSCs. Additionally, thus far we have only looked at gene expression changes for Ing4$^{-/-}$ HSCs as a combined group compared to wild type. Identifying pathways that are differentially expressed between Ing4$^{-/-}$ LT- and ST-HSCs may guide in understanding some of the observed differences. Nevertheless, we have identified several compelling phenotypes that warrant further exploration.

In summary, our work demonstrates a unique model where genetic deletion of Ing4 triggers HSCs to maintain quiescence despite transcriptional upregulation of activation markers. This model may provide target pathways for limiting translational activation of HSCs to prevent exhaustion. Manipulation of these pathways may provide a powerful mechanism to improve HSC function during hematopoietic stress.

## STAR★METHODS

Detailed methods are provided in the online version of this paper and include the following:

- KEY RESOURCES TABLE
- RESOURCE AVAILABILITY
  - Lead contact
  - Materials availability
  - Data and code availability
- EXPERIMENTAL MODEL AND STUDY PARTICIPANT DETAILS
  - Mice
- METHOD DETAILS
  - Bone marrow and peripheral blood preparation
  - Flow cytometry
  - Cell cycle analysis
  - Reactive oxygen species analysis
  - Senescence assay
  - RNA-seq analysis
  - Quantitative real-time PCR
  - Transplantation assays
  - Cell proliferation assay
  - 5-Fluorouracil treatment
  - c-Myc inhibition
- QUANTIFICATION AND STATISTICAL ANALYSIS

## SUPPLEMENTAL INFORMATION

Supplemental information can be found online at https://doi.org/10.1016/j.isci.2024.110521.

## ACKNOWLEDGMENTS

This work was funded by NIH R03DK12438-01, NIH K01DK104974-01, NIH 5P20GM109091-05, and USC ASPIRE 130100-24-68351. We would like to thank the Flow Cytometry Core Facilities at the University of South Carolina (UofSC) School of Pharmacy. Specifically, we thank Chang-Uk Lim for his assistance with flow cytometry sorting, analysis, and experimental design. We also thank Jason Kubinak and Kia Zellars for their assistance in using the Instrumentation Resource Facility flow cytometer at the UofSC School of Medicine. For animal support, we thank the University of South Carolina Department of Laboratory Animal Research core members Shaun Thacker and Marlee Poole.

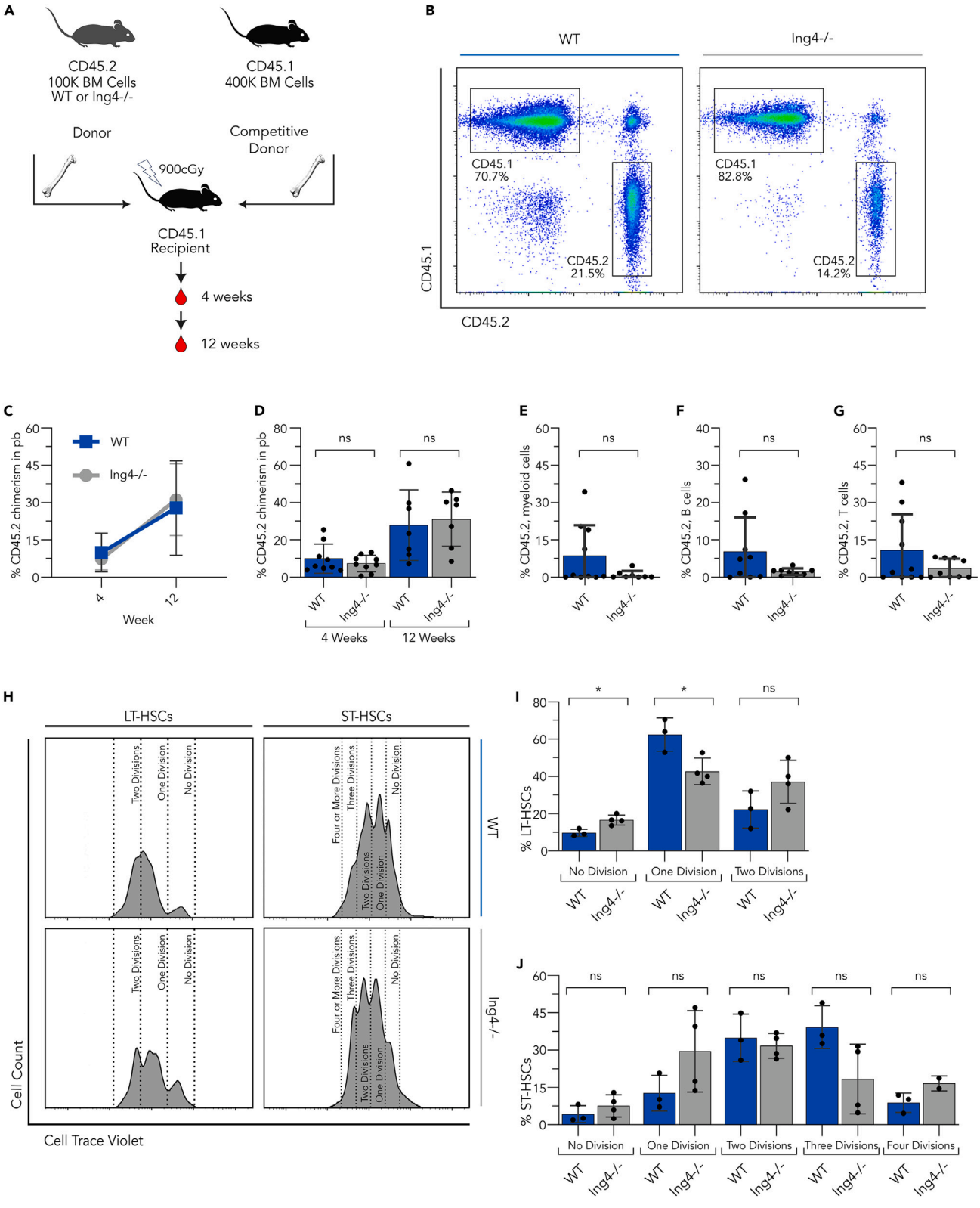
A
CD45.2
100K BM Cells
WT or Ing4-/-
CD45.1
400K BM Cells
Donor
Competitive
Donor
900cGy
CD45.1
Recipient
4 weeks
12 weeks
B
WT
Ing4-/-
CD45.1
70.7%
CD45.2
21.5%
CD45.1
82.8%
CD45.2
14.2%
CD45.1
CD45.2
C
% CD45.2 chimerism in pb
WT
Ing4-/-
Week
D
% CD45.2 chimerism in pb
ns
4 Weeks
12 Weeks
E
% CD45.2, myeloid cells
F
% CD45.2, B cells
G
% CD45.2, T cells
H
LT-HSCs
ST-HSCs
Two Divisions
One Division
No Division
Four or More Divisions
Three Divisions
WT
Ing4-/-
Cell Count
Cell Trace Violet
I
% LT-HSCs
No Division
One Division
Two Divisions
J
% ST-HSCs
Three Divisions
Four Divisions

**Figure 5. In competitive whole bone marrow transplantation assays, Ing4$^{-/-}$ cells contribute to chimerism at levels comparable to WT**

(A) Schematic overview of the competitive transplantation assay using WBM from WT and Ing4$^{-/-}$ mice.

(B) Representative flow cytometric analysis of CD45.1 and CD45.2 chimerism in peripheral blood collected from recipient mice 12 weeks following transplantation with WBM from WT and Ing4$^{-/-}$ mice.

(C) Mean and standard deviation depicting percentages of CD45.2 chimerism in the peripheral blood of recipient mice collected 4 and 12 weeks following competitive WBM transplantation. ($n$ = 7–9).

(D) CD45.2 chimerism in individual mice from the peripheral blood of recipient mice collected 4 and 12 weeks following competitive WBM transplantation. ($n$ = 7–9; ns = $p > 0.05$).

(E) CD45.2 chimerism of myeloid cells in the peripheral blood of recipient mice collected 12 weeks following competitive WBM transplantation. ($n$ = 8–10; ns = $p > 0.05$).

(F) CD45.2 chimerism of B-cells in the peripheral blood of recipient mice collected 12 weeks following competitive WBM transplantation. ($n$ = 8–10; ns = $p > 0.05$).

(G) CD45.2 chimerism of T cells in the peripheral blood of recipient mice collected 12 weeks following competitive WBM transplantation. ($n$ = 8–10; ns = $p > 0.05$).

(H) Representative flow cytometric analysis using CellTrace Violet to show cell division events for 7 days culture.

(I) Proliferation assay quantifying cell division events for LT-HSCs for 7 days in culture. ($n$ = 3–4; ns = $p > 0.05$; *$p < 0.05$).

(J) Proliferation assay quantifying cell division events for ST-HSCs undergoing no, one, two, three or four cell divisions in 7 days ($n$ = 3–4; ns = $p > 0.05$).

Data in (E), (F), (G), (I), and (J) reflect mean values ±SD. Statistical significance was assessed using Student's t test with Welch's correction.

## AUTHOR CONTRIBUTIONS

Conceptualization, K.L.K. and Z.T.; methodology, K.L.K., Z.T., G.A., M.R., M.H., C.A.Q., S.G., A.M., and V.B.; data analysis, K.L.K., Z.T., G.A., M.H., C.A.Q., A.M., V.B., and A.M.T.; writing, K.L.K., Z.T., and G.A.; funding acquisition, K.L.K.; supervision, K.L.K.

## DECLARATION OF INTERESTS

The authors declare no competing interests.

Received: March 15, 2023
Revised: May 14, 2024
Accepted: July 12, 2024
Published: July 15, 2024

## REFERENCES

1. Orkin, S., and Zon, L. (2008). Hematopoiesis: an evolving paradigm for stem cell biology. Cell *132*, 631–644. https://doi.org/10.1016/j.cell.2008.01.025.
2. Kondo, M., Wagers, A.J., Manz, M.G., Prohaska, S.S., Scherer, D.C., Beilhack, G.F., Shizuru, J.A., and Weissman, I.L. (2003). Biology of hematopoietic stem cells and progenitors: implications for clinical application. Annu. Rev. Immunol. *21*, 759–806. https://doi.org/10.1146/annurev.immunol.21.120601.141007.
3. Kiel, M.J., and Morrison, S.J. (2006). Maintaining hematopoietic stem cells in the vascular niche. Immunity *25*, 862–864. https://doi.org/10.1016/j.immuni.2006.11.005.
4. Trumpp, A., Essers, M., and Wilson, A. (2010). Awakening dormant haematopoietic stem cells. Nat. Rev. Immunol. *10*, 201–209. https://doi.org/10.1038/nri2726.
5. Wilson, A., and Trumpp, A. (2006). Bone-marrow haematopoietic-stem-cell niches. Nat. Rev. Immunol. *6*, 93–106. https://doi.org/10.1038/nri1779.
6. Yamada, T., Park, C.S., and Lacorazza, H.D. (2013). Genetic control of quiescence in hematopoietic stem cells. Cell Cycle *12*, 2376–2383. https://doi.org/10.4161/cc.25416.
7. Matsumoto, A., Takeishi, S., Kanie, T., Susaki, E., Onoyama, I., Tateishi, Y., Nakayama, K., and Nakayama, K.I. (2011). P57 Is required for quiescence and maintenance of adult hematopoietic stem cells. Cell Stem Cell *9*, 262–271. https://doi.org/10.1016/j.stem.2011.06.014.
8. Bernstein, B.E., Kamal, M., Lindblad-Toh, K., Bekiranov, S., Bailey, D.K., Huebert, D.J., McMahon, S., Karlsson, E.K., Kulbokas, E.J., Gingeras, T.R., et al. (2005). Genomic maps and comparative analysis of histone modifications in human and mouse. Cell *120*, 169–181. https://doi.org/10.1016/j.cell.2005.01.001.
9. Claus, R., and Lübbert, M. (2003). Epigenetic targets in hematopoietic malignancies. Oncogene *22*, 6489–6496. https://doi.org/10.1038/sj.onc.1206814.
10. Friedman, A.D. (2007). Transcriptional control of granulocyte and monocyte development. Oncogene *26*, 6816–6828. https://doi.org/10.1038/sj.onc.1210764.
11. Gallipoli, P., Giotopoulos, G., and Huntly, B.J.P. (2015). Epigenetic regulators as promising therapeutic targets in acute myeloid leukemia. Ther. Adv. Hematol. *6*, 103–119. https://doi.org/10.1177/2040620715577614.
12. Hsia, N., and Zon, L.I. (2005). Transcriptional regulation of hematopoietic stem cell development in zebrafish. Exp. Hematol. *33*, 1007–1014. https://doi.org/10.1016/j.exphem.2005.06.013.
13. Huang, H.T., Kathrein, K.L., Barton, A., Gitlin, Z., Huang, Y.H., Ward, T.P., Hofmann, O., Dibiase, A., Song, A., Tyekucheva, S., et al. (2013). A Network of Epigenetic Regulators Guides Developmental Haematopoiesis in Vivo. Nat. Cell Biol. *15*, 1516–1525. https://doi.org/10.1038/ncb2870.
14. McKinney-Freeman, S., Cahan, P., Li, H., Lacadie, S.A., Huang, H.T., Curran, M., Loewer, S., Naveiras, O., Kathrein, K.L., Konantz, M., et al. (2012). The transcriptional landscape of hematopoietic stem cell ontogeny. Cell Stem Cell *11*, 701–714. https://doi.org/10.1016/j.stem.2012.07.018.
15. Rice, K.L., Hormaeche, I., and Licht, J.D. (2007). Epigenetic regulation of normal and malignant hematopoiesis. Oncogene *26*, 6697–6714. https://doi.org/10.1038/sj.onc.1210755.
16. Dykstra, B., Kent, D., Bowie, M., McCaffrey, L., Hamilton, M., Lyons, K., Lee, S.J., Brinkman, R., and Eaves, C. (2007). Long-Term Propagation of Distinct Hematopoietic Differentiation Programs In Vivo. Cell Stem Cell *1*, 218–229. https://doi.org/10.1016/j.stem.2007.05.015.
17. Anderson, G.A., Rodriguez, M., and Kathrein, K.L. (2020). Regulation of stress-induced hematopoiesis. Curr. Opin. Hematol. *27*, 279–287. https://doi.org/10.1097/MOH.0000000000000589.
18. Olson, O.C., Kang, Y.A., and Passegué, E. (2020). Normal hematopoiesis is a balancing act of self-renewal and regeneration. Cold Spring Harb. Perspect Med. *10*, 1–23. https://doi.org/10.1101/cshperspect.a035519.
19. Rodríguez, A., Zhang, K., Färkkilä, A., Filiatrault, J., Yang, C., Velázquez, M., Furutani, E., Goldman, D.C., García de Teresa, B., Garza-Mayén, G., et al. (2021).

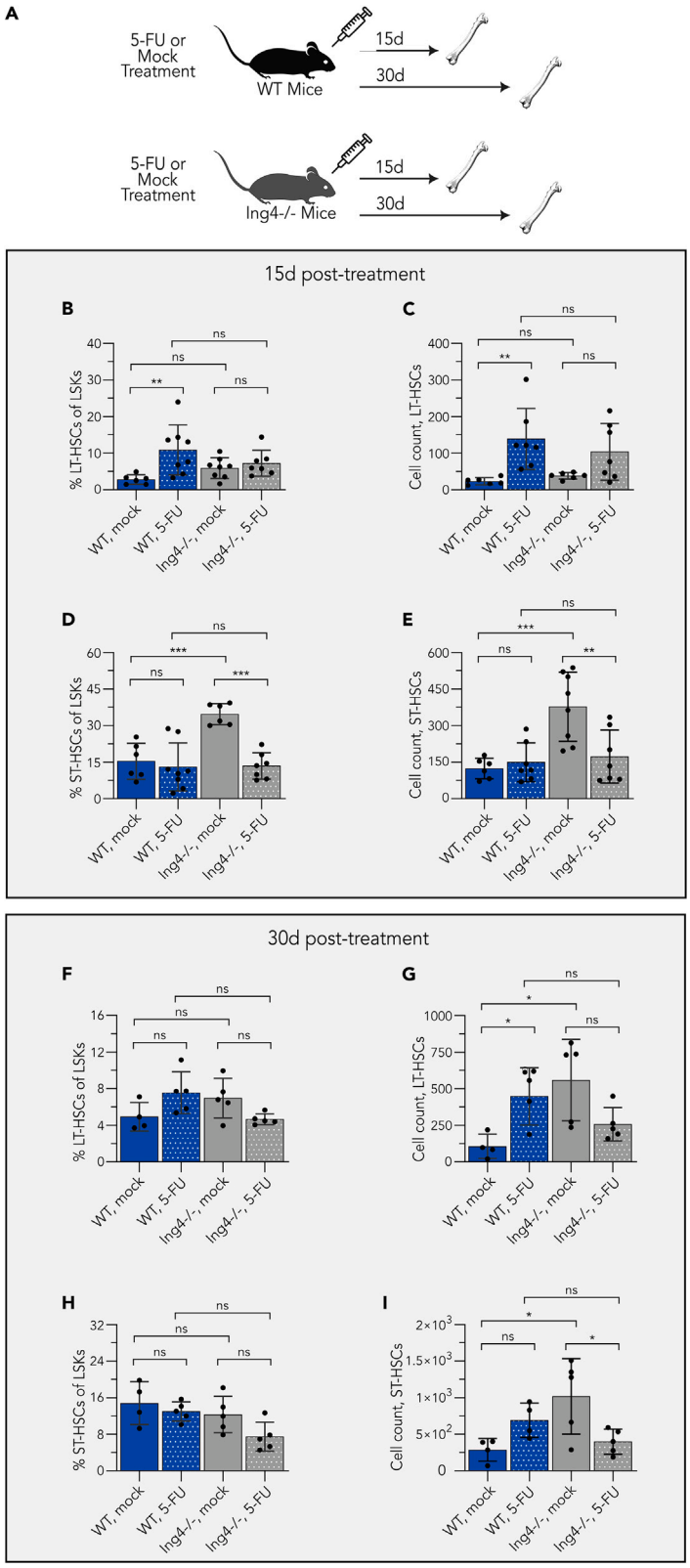
A
5-FU or Mock Treatment
WT Mice
15d
30d
5-FU or Mock Treatment
Ing4-/- Mice
15d
30d
15d post-treatment
B
% LT-HSCs of LSKs
C
Cell count, LT-HSCs
D
% ST-HSCs of LSKs
E
Cell count, ST-HSCs
30d post-treatment
F
% LT-HSCs of LSKs
G
Cell count, LT-HSCs
H
% ST-HSCs of LSKs
I
Cell count, ST-HSCs
WT, mock
WT, 5-FU
Ing4-/-, mock
Ing4-/-, 5-FU
ns

**Figure 6. Ing4-deficient HSCs show altered stress hematopoiesis following chemotoxic insult**

(A) Schematic overview of the 5-FU assay in WT and Ing4$^{-/-}$ mice.

(B) LT-HSCs isolated from individual 5-FU or mock treated WT and Ing4$^{-/-}$ mice, as a percentage of the LSK population at 15 days post-treatment. ($n$ = 6–8; ns = $p > 0.05$; ** = $p < 0.01$).

(C) Cell count of LT-HSCs isolated from individual 5-FU or mock treated WT and Ing4$^{-/-}$ mice, at 15 days post-treatment. ($n$ = 5–6; ns = $p > 0.05$; ** = $p < 0.01$).

(D) ST-HSCs isolated from individual 5-FU or mock treated WT and Ing4$^{-/-}$ mice, as a percentage of the LSK population at 15 days post-treatment. ($n$ = 6–8; ns = $p > 0.05$; *** = $p < 0.005$).

(E) Cell count of ST-HSCs isolated from individual 5-FU or mock treated WT and Ing4$^{-/-}$ mice, at 15 days post-treatment. ($n$ = 4–5; ns = $p > 0.05$; ** = $p < 0.01$; *** = $p < 0.005$).

(F) LT-HSCs isolated from individual 5-FU or mock treated WT and Ing4$^{-/-}$ mice, as a percentage of the LSK population at 30 days post-treatment. ($n$ = 6–8; ns = $p > 0.05$).

(G) Cell count of LT-HSCs isolated from individual 5-FU or mock treated WT and Ing4$^{-/-}$ mice, at 30 days post-treatment. ($n$ = 6–8; ns = $p > 0.05$; * = $p < 0.05$).

(H) ST-HSCs isolated from individual 5-FU or mock treated WT and Ing4$^{-/-}$ mice treated, as a percentage of the LSK population at 30 days post-treatment. ($n$ = 6–8; ns = $p > 0.05$).

(I) Cell count of ST-HSCs isolated from individual 5-FU or mock treated WT and Ing4$^{-/-}$ mice, at 30 days post-treatment. ($n$ = 4–5; ns = $p > 0.05$; * = $p < 0.05$).

Data in (B), (C), (D), (E), (F), (G), (H), and (I) reflect mean values ± SD. Statistical significance was assessed using a two-way ANOVA analysis followed by Tukey's post hoc test.

MYC Promotes Bone Marrow Stem Cell Dysfunction in Fanconi Anemia. Cell Stem Cell *28*, 33–47.e8. https://doi.org/10.1016/j.stem.2020.09.004.

20. Matatall, K.A., Jeong, M., Chen, S., Sun, D., Chen, F., Mo, Q., Kimmel, M., and King, K.Y. (2016). Chronic Infection Depletes Hematopoietic Stem Cells through Stress-Induced Terminal Differentiation. Cell Rep. *17*, 2584–2595. https://doi.org/10.1016/j.celrep.2016.11.031.
21. Mahmoud, H.K., Elhaddad, A.M., Fahmy, O.A., Samra, M.A., Abdelfattah, R.M., El-Nahass, Y.H., Fathy, G.M., and Abdelhady, M.S. (2015). Allogeneic hematopoietic stem cell transplantation for non-malignant hematological disorders. J. Adv. Res. *6*, 449–458. https://doi.org/10.1016/j.jare.2014.11.001.
22. Cui, S., Gao, Y., Zhang, K., Chen, J., Wang, R., and Chen, L. (2015). The emerging role of inhibitor of growth 4 as a tumor suppressor in multiple human cancers. Cell. Physiol. Biochem. *36*, 409–422. https://doi.org/10.1159/000430108.
23. Fang, F., Luo, L.B., Tao, Y.M., Wu, F., and Yang, L.Y. (2009). Decreased expression of inhibitor of growth 4 correlated with poor prognosis of hepatocellular carcinoma. Cancer Epidemiol. Biomarkers Prev. *18*, 409–416. https://doi.org/10.1158/1055-9965.EPI-08-0575.
24. Moreno, A., Palacios, A., Orgaz, J.L., Jimenez, B., Blanco, F.J., and Palmero, I. (2010). Functional impact of cancer-associated mutations in the tumor suppressor protein ING4. Carcinogenesis *31*, 1932–1938. https://doi.org/10.1093/carcin/bgq171.
25. Uhlén, M., Fagerberg, L., Hallström, B.M., Lindskog, C., Oksvold, P., Mardinoglu, A., Sivertsson, Å., Kampf, C., Sjöstedt, E., Asplund, A., et al. (2015). Tissue-based map of the human proteome. Science *347*, XX. https://doi.org/10.1126/science.1260419.
26. Shiseki, M., Nagashima, M., Pedeux, R.M., Kitahama-Shiseki, M., Miura, K., Okamura, S., Onogi, H., Higashimoto, Y., Appella, E., Yokota, J., and Harris, C.C. (2003). p29ING4 and p28ING5 Bind to p53 and p300, and Enhance p53 Activity. Cancer Res. *63*, 2373–2378.
27. Doyon, Y., Cayrou, C., Ullah, M., Landry, A.J., Côté, V., Selleck, W., Lane, W.S., Tan, S., Yang, X.J., and Côté, J. (2006). ING tumor suppressor proteins are critical regulators of chromatin acetylation required for genome expression and perpetuation. Mol. Cell *21*, 51–64. https://doi.org/10.1016/j.molcel.2005.12.007.
28. Palacios, A., Munoz, I.G., Pantoja-Uceda, D., Marcaida, M.J., Torres, D., Martin-Garcia, J.M., Luque, I., Montoya, G., and Blanco, F.J. (2008). Molecular basis of histone H3K4me3 recognition by ING4. J. Biol. Chem. *283*, 15956–15964. https://doi.org/10.1074/jbc.M710020200.
29. Garkavtsev, I., Kozin, S.V., Chernova, O., Xu, L., Winkler, F., Brown, E., Barnett, G.H., and Jain, R.K. (2004). The candidate tumour suppressor protein ING4 regulates brain tumour growth and angiogenesis. Nature *428*, 328–332. https://doi.org/10.1038/nature02329.
30. Li, S., Fan, T., Liu, H., Chen, J., Qin, C., and Ren, X. (2013). Tumor suppressor ING4 overexpression contributes to proliferation and invasion inhibition in gastric carcinoma by suppressing the NF-κB signaling pathway. Mol. Biol. Rep. *40*, 5723–5732. https://doi.org/10.1007/s11033-013-2675-3.
31. Byron, S.A., Min, E., Thal, T.S., Hostetter, G., Watanabe, A.T., Azorsa, D.O., Little, T.H., Tapia, C., and Kim, S. (2012). Negative Regulation of NF-κB by the ING4 Tumor Suppressor in Breast Cancer. PLoS One *7*, e46823. https://doi.org/10.1371/journal.pone.0046823.
32. Coles, A.H., Gannon, H., Cerny, A., Kurt-Jones, E., and Jones, S.N. (2010). Inhibitor of growth-4 promotes IkappaB promoter activation to suppress NF-kappaB signaling and innate immunity. Proc. Natl. Acad. Sci. USA *107*, 11423–11428. https://doi.org/10.1073/pnas.0912116107.
33. Mathema, V.B., and Koh, Y.-S. (2012). Inhibitor of growth-4 mediates chromatin modification and has a suppressive effect on tumorigenesis and innate immunity. Tumour Biol. *33*, 1–7. https://doi.org/10.1007/s13277-011-0249-3.
34. Lu, M., Pan, C., Zhang, L., Ding, C., Chen, F., Wang, Q., Wang, K., and Zhang, X. (2013). ING4 inhibits the translation of proto-oncogene MYC by interacting with AUF1. FEBS Lett. *587*, 1597–1604. https://doi.org/10.1016/j.febslet.2013.04.004.
35. Ozer, A., Wu, L.C., and Bruick, R.K. (2005). The candidate tumor suppressor ING4 represses activation of the hypoxia inducible factor (HIF). Proc. Natl. Acad. Sci. USA *102*, 7481–7486. https://doi.org/10.1073/pnas.0502716102.
36. Guo, Y., Meng, X., Wang, Q., Wang, Y., and Shang, H. (2013). The ING4 Binding with p53 and Induced p53 Acetylation were Attenuated by Human Papillomavirus 16 E6. PLoS One *8*, e71453. https://doi.org/10.1371/journal.pone.0071453.
37. Bagger, F.O., Kinalis, S., and Rapin, N. (2019). BloodSpot: A database of healthy and malignant haematopoiesis updated with purified and single cell mRNA sequencing profiles. Nucleic Acids Res. *47*, D881–D885. https://doi.org/10.1093/nar/gky1076.
38. Bagger, F.O., Sasivarevic, D., Sohi, S.H., Laursen, L.G., Pundhir, S., Sønderby, C.K., Winther, O., Rapin, N., and Porse, B.T. (2016). BloodSpot: A database of gene expression profiles and transcriptional programs for healthy and malignant haematopoiesis. Nucleic Acids Res. *44*, D917–D924. https://doi.org/10.1093/nar/gkv1101.
39. Kiel, M.J., Yilmaz, O.H., and Morrison, S.J. (2008). CD150− cells are transiently reconstituting multipotent progenitors with little or no stem cell activity. Blood *111*, 4413–4415.
40. Orford, K.W., and Scadden, D.T. (2008). Deconstructing stem cell self-renewal: genetic insights into cell-cycle regulation. Nat. Rev. Genet. *9*, 115–128.
41. Pietras, E.M., Warr, M.R., and Passegue, E. (2011). Cell cycle regulation in hematopoietic stem cells. J. Cell Biol. *195*, 709–720. https://doi.org/10.1083/jcb.201102131.
42. Yang, L., Bryder, D., Adolfsson, J., Nygren, J., Mansson, R., Sigvardsson, M., and Jacobsen, S.E.W. (2005). Identification of Lin–Sca1+ kit+ CD34+ Flt3–short-term hematopoietic stem cells capable of rapidly reconstituting and rescuing myeloablated transplant recipients. Blood *105*, 2717–2723.
43. Osawa, M., Hanada, K., Hamada, H., and Nakauchi, H. (1996). Long-term lymphohematopoietic reconstitution by a single CD34-low/negative hematopoietic stem cell. Science *273*, 242–245. https://doi.org/10.1126/science.273.5272.242.
44. Pietras, E.M., Reynaud, D., Kang, Y.A., Carlin, D., Calero-Nieto, F.J., Leavitt, A.D., Stuart, J.M., Gottgens, B., and Passegue, E. (2015). Functionally Distinct Subsets of Lineage-Biased Multipotent Progenitors Control Blood Production in Normal and Regenerative Conditions. Cell Stem Cell *17*,

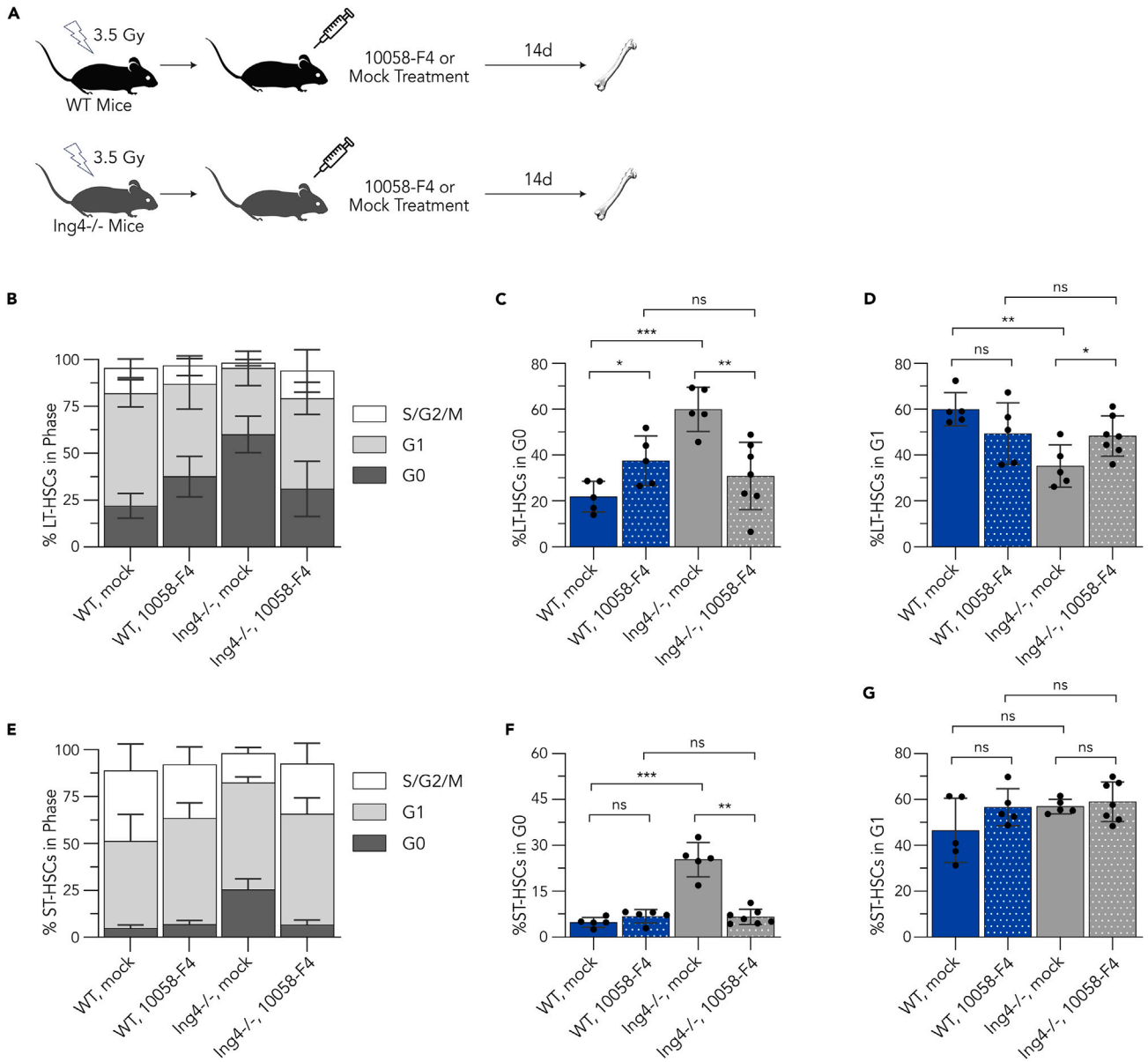


**Figure 7. Inhibition of c-Myc activity induces cell cycling in Ing4$^{-/-}$ HSCs after low-dose irradiation**

(A) Schematic overview of the c-Myc inhibitor assay in WT and Ing4$^{-/-}$ mice.

(B) Mean values and standard deviations of all cell cycle phases for mock or 10058-F4 treated LT-HSCs in WT and Ing4$^{-/-}$ mice, as a percentage of LT-HSC population. ($n$ = 5).

(C) LT-HSCs in $G_0$ from individual mock or 10058-F4 treated WT and Ing4$^{-/-}$ mice, as a percentage of the LT-HSC population. ($n$ = 5; ns = $p > 0.05$; *$p < 0.05$; **$p < 0.01$; *** = $p < 0.005$).

(D) LT-HSCs in $G_1$ from individual mock or 10058-F4 treated WT and Ing4$^{-/-}$ mice, as a percentage of the LT-HSC population. ($n$ = 5; ns = $p > 0.05$; *$p < 0.05$; **$p < 0.01$).

(E) Mean values and standard deviations of all cell cycle phases for individual mock or 10058-F4 treated ST-HSCs in WT and Ing4$^{-/-}$ mice, as a percentage of ST-HSC population. ($n$ = 5).

(F) ST-HSCs in $G_0$ from individual mock or 10058-F4 treated WT and Ing4$^{-/-}$ mice, as a percentage of the ST-HSC population. ($n$ = 5; ns = $p > 0.05$; **$p < 0.01$; *** = $p < 0.005$).

(G) ST-HSCs in $G_1$ from individual mock or 10058-F4 treated WT and Ing4$^{-/-}$ mice, as a percentage of the ST-HSC population. ($n$ = 5; ns = $p > 0.05$).

Data in (C), (D), (F), and (G) reflect mean values ± SD. Statistical significance was assessed using a two-way ANOVA followed by Tukey's post hoc test. Total cell counts for LT- and ST-HSCs are shown in Figures S4A and S4B.

35–46. https://doi.org/10.1016/j.stem.2015.05.003.

45. Sommerkamp, P., Romero-Mulero, M.C., Narr, A., Ladel, L., Hustin, L., Schonberger, K., Renders, S., Altamura, S., Zeisberger, P., Jacklein, K., et al. (2021). Mouse multipotent progenitor 5 cells are located at the interphase between hematopoietic stem and progenitor cells. Blood *137*, 3218–3224. https://doi.org/10.1182/blood.2020007876.
46. Pietras, E.M. (2017). Inflammation: a key regulator of hematopoietic stem cell fate in health and disease. Blood *130*, 1693–1698. https://doi.org/10.1182/blood-2017-06-780882.
47. Zhang, X., Wang, K.S., Wang, Z.Q., Xu, L.S., Wang, Q.W., Chen, F., Wei, D.Z., and Han, Z.G. (2005). Nuclear localization signal of ING4 plays a key role in its binding to p53. Biochem. Biophys. Res. Commun. *331*, 1032–1038. https://doi.org/10.1016/j.bbrc.2005.04.023.
48. Jang, Y.Y., and Sharkis, S.J. (2007). A low level of reactive oxygen species selects for primitive hematopoietic stem cells that may reside in the low-oxygenic niche. Blood *110*, 3056–3063. https://doi.org/10.1182/blood-2007-05-087759.
49. Shao, L., Li, H., Pazhanisamy, S.K., Meng, A., Wang, Y., and Zhou, D. (2011). Reactive oxygen species and hematopoietic stem cell senescence. Int. J. Hematol. *94*, 24–32. https://doi.org/10.1007/s12185-011-0872-1.
50. Hsu, P., and Qu, C.K. (2013). Metabolic plasticity and hematopoietic stem cell biology. Curr. Opin. Hematol. *20*, 289–294. https://doi.org/10.1097/MOH.0b013e328360ab4d.
51. Simsek, T., Kocabas, F., Zheng, J., Deberardinis, R.J., Mahmoud, A.I., Olson, E.N., Schneider, J.W., Zhang, C.C., and Sadek, H.A. (2010). The distinct metabolic profile of hematopoietic stem cells reflects their location in a hypoxic niche. Cell Stem Cell *7*, 380–390. https://doi.org/10.1016/j.stem.2010.07.011.
52. Berger, P.L., Frank, S.B., Schulz, V.V., Nollet, E.A., Edick, M.J., Holly, B., Chang, T.T.A., Hostetter, G., Kim, S., and Miranti, C.K. (2014). Transient induction of ING4 by Myc drives prostate epithelial cell differentiation and its disruption drives prostate tumorigenesis. Cancer Res. *74*, 3357–3368. https://doi.org/10.1158/0008-5472.CAN-13-3076.
53. Huang, M.J., Cheng, Y.C., Liu, C.R., Lin, S., and Liu, H.E. (2006). A small-molecule c-Myc inhibitor, 10058-F4, induces cell-cycle arrest, apoptosis, and myeloid differentiation of human acute myeloid leukemia. Exp. Hematol. *34*, 1480–1489. https://doi.org/10.1016/j.exphem.2006.06.019.
54. Scognamiglio, R., Cabezas-Wallscheid, N., Thier, M.C., Altamura, S., Reyes, A., Prendergast, A.M., Baumgartner, D., Carnevalli, L.S., Atzberger, A., Haas, S., et al. (2016). Myc Depletion Induces a Pluripotent Dormant State Mimicking Diapause. Cell *164*, 668–680. https://doi.org/10.1016/j.cell.2015.12.033.
55. Mapperley, C., van de Lagemaat, L.N., Lawson, H., Tavosanis, A., Paris, J., Campos, J., Wotherspoon, D., Durko, J., Sarapuu, A., Choe, J., et al. (2021). The mRNA m6A reader YTHDF2 suppresses proinflammatory pathways and sustains hematopoietic stem cell function. J. Exp. Med. *218*, e20200829. https://doi.org/10.1084/jem.20200829.
56. Cabezas-Wallscheid, N., Buettner, F., Sommerkamp, P., Klimmeck, D., Ladel, L., Thalheimer, F.B., Pastor-Flores, D., Roma, L.P., Renders, S., Zeisberger, P., et al. (2017). Vitamin A-Retinoic Acid Signaling Regulates Hematopoietic Stem Cell Dormancy. Cell *169*, 807–823.e19. https://doi.org/10.1016/j.cell.2017.04.018.
57. Fan, C., Zhao, C., Zhang, F., Kesarwani, M., Tu, Z., Cai, X., Davis, A.K., Xu, L., Hochstetler, C.L., Chen, X., et al. (2021). Adaptive responses to mTOR gene targeting in hematopoietic stem cells reveal a proliferative mechanism evasive to mTOR inhibition. Proc. Natl. Acad. Sci. USA *118*, e2020102118. https://doi.org/10.1073/pnas.2020102118/-/DCSupplemental.
58. Sommerkamp, P., Romero-Mulero, M.C., Narr, A., Ladel, L., Hustin, L., Schonberger, K., Renders, S., Altamura, S., Zeisberger, P., Jacklein, K., et al. (2021). Mouse multipotent progenitor 5 cells are located at the interphase between hematopoietic stem and progenitor cells. Blood *137*, 3218–3224.
59. Spevak, C.C., Elias, H.K., Kannan, L., Ali, M.A.E., Martin, G.H., Selvaraj, S., Eng, W.S., Ernlund, A., Rajasekhar, V.K., Woolthuis, C.M., et al. (2020). Hematopoietic Stem and Progenitor Cells Exhibit Stage-Specific Translational Programs via mTOR- and CDK1-Dependent Mechanisms. Cell Stem Cell *26*, 755–765.e7. https://doi.org/10.1016/j.stem.2019.12.006.
60. van Velthoven, C.T.J., and Rando, T.A. (2019). Stem Cell Quiescence: Dynamism, Restraint, and Cellular Idling. Cell Stem Cell *24*, 213–225. https://doi.org/10.1016/j.stem.2019.01.001.
61. Kaufmann, K.B., Zeng, A.G.X., Coyaud, E., Garcia-Prat, L., Papalexi, E., Murison, A., Laurent, E.M.N., Chan-Seng-Yue, M., Gan, O.I., Pan, K., et al. (2021). A latent subset of human hematopoietic stem cells resists regenerative stress to preserve stemness. Nat. Immunol. *22*, 723–734. https://doi.org/10.1038/s41590-021-00925-1.
62. Zhang, Y.W., Mess, J., Aizarani, N., Mishra, P., Johnson, C., Romero-Mulero, M.C., Rettkowski, J., Schönberger, K., Obier, N., Jäcklein, K., et al. (2022). Hyaluronic acid–GPRC5C signalling promotes dormancy in haematopoietic stem cells. Nat. Cell Biol. *24*, 1038–1048. https://doi.org/10.1038/s41556-022-00931-x.
63. Ali, M.A.E., Fuse, K., Tadokoro, Y., Hoshii, T., Ueno, M., Kobayashi, M., Nomura, N., Vu, H.T., Peng, H., Hegazy, A.M., et al. (2017). Functional dissection of hematopoietic stem cell populations with a stemness-monitoring system based on NS-GFP transgene expression. Sci. Rep. *7*, 11442. https://doi.org/10.1038/s41598-017-11909-3.
64. Joaquin, M., Gubern, A., González-Nuñez, D., Josué Ruiz, E., Ferreiro, I., De Nadal, E., Nebreda, A.R., and Posas, F. (2012). The p57 CDKi integrates stress signals into cell-cycle progression to promote cell survival upon stress. EMBO J. *31*, 2952–2964. https://doi.org/10.1038/emboj.2012.122.
65. Min, I.M., Pietramaggiori, G., Kim, F.S., Passegué, E., Stevenson, K.E., and Wagers, A.J. (2008). The Transcription Factor EGR1 Controls Both the Proliferation and Localization of Hematopoietic Stem Cells. Cell Stem Cell *2*, 380–391. https://doi.org/10.1016/j.stem.2008.01.015.
66. Nachmani, D., Bothmer, A.H., Grisendi, S., Mele, A., Bothmer, D., Lee, J.D., Monteleone, E., Cheng, K., Zhang, Y., Bester, A.C., et al. (2019). Germline NPM1 mutations lead to altered rRNA 2′-O-methylation and cause dyskeratosis congenita. Nat. Genet. *51*, 1518–1529. https://doi.org/10.1038/s41588-019-0502-z.
67. Park, I.-K., Qian, D., Kiel, M., Becker, M.W., Pihalja, M., Weissman, I.L., Morrison, S.J., and Clarke, M.F. (2003). Bmi-1 is required for maintenance of adult self-renewing haematopoietic stem cells. Nature *423*, 302–305.
68. Park, I.-K., He, Y., Lin, F., Laerum, O.D., Tian, Q., Bumgarner, R., Klug, C.A., Li, K., Kuhr, C., Doyle, M.J., et al. (2002). Differential gene expression profiling of adult murine hematopoietic stem cells. Blood *99*, 488–498.
69. Tsai, F.-Y., Kellert, G., Kuo, F.C., Weiss, M., Chen, J., Rosenblatt, M., Altt, F.W., and Orkin, S.H. (1994). An early haematopoietic defect in mice lacking the transcription factor GATA-2. Nature *371*, 221–226.
70. Zou, P., Yoshihara, H., Hosokawa, K., Tai, I., Shinmyozu, K., Tsukahara, F., Maru, Y., Nakayama, K., Nakayama, K.I., and Suda, T. (2011). P57 Kip2 and p27 Kip1 cooperate to maintain hematopoietic stem cell quiescence through interactions with Hsc70. Cell Stem Cell *9*, 247–261. https://doi.org/10.1016/j.stem.2011.07.003.
71. Pietras, E.M., Lakshminarasimhan, R., Techner, J.M., Fong, S., Flach, J., Binnewies, M., and Passegue, E. (2014). Re-entry into quiescence protects hematopoietic stem cells from the killing effect of chronic exposure to type I interferons. J. Exp. Med. *211*, 245–262. https://doi.org/10.1084/jem.20131043.
72. Wilson, A., Murphy, M.J., Oskarsson, T., Kaloulis, K., Bettess, M.D., Oser, G.M., Pasche, A.C., Knabenhans, C., MacDonald, H.R., and Trumpp, A. (2004). c-Myc controls the balance between hematopoietic stem cell self-renewal and differentiation. Genes Dev. *18*, 2747–2763. https://doi.org/10.1101/gad.313104.
73. Reavie, L., Della Gatta, G., Crusio, K., Aranda-Orgilles, B., Buckley, S.M., Thompson, B., Lee, E., Gao, J., Bredemeyer, A.L., Helmink, B.A., et al. (2010). Regulation of hematopoietic stem cell differentiation by a single ubiquitin ligase-substrate complex. Nat. Immunol. *11*, 207–215. https://doi.org/10.1038/ni.1839.
74. La, T., Chen, S., Guo, T., Zhao, X.H., Teng, L., Li, D., Carnell, M., Zhang, Y.Y., Feng, Y.C., Cole, N., et al. (2021). Visualization of endogenous p27 and Ki67 reveals the importance of a c-Myc-driven metabolic switch in promoting survival of quiescent cancer cells. Theranostics *11*, 9605–9622. https://doi.org/10.7150/THNO.63763.
75. Sheng, Y., Ma, R., Yu, C., Wu, Q., Zhang, S., Paulsen, K., Zhang, J., Ni, H., Huang, Y., Zheng, Y., and Qian, Z. (2021). Role of c-Myc haploinsufficiency in the maintenance of HSCs in mice. Blood *137*, 610–623.
76. Laurenti, E., Varnum-Finney, B., Wilson, A., Ferrero, I., Blanco-Bose, W., Ehninger, A., Knoepfler, P., Cheng, P.-F., MacDonald, H., Eisenman, R., et al. (2008). Hematopoietic stem cell function and survival depend on c-Myc and N-Myc activity. Cell Stem Cell *3*, 611–624. https://doi.org/10.1016/j.stem.2008.09.005.
77. Aksoz, M., Albayrak, E., Servet, G., Raife, A., Turan, D., Yazgi, L., Pinar, A., Emre, S., Tuysuz,

C., Canikyan, S., et al. (2019). c-Myc Inhibitor 10074-G5 Induces Murine and Human Hematopoietic Stem and Progenitor Cell Expansion and HDR Modulator Rad51 Expression. Curr. Cancer Drug Targets *19*, 479–494.

78. Jarzebowski, L., Le Bouteiller, M., Coqueran, S., Raveux, A., Vandormael-Pournin, S., David, A., Cumano, A., and Cohen-Tannoudji, M. (2018). Mouse adult hematopoietic stem cells actively synthesize ribosomal RNA. RNA *24*, 1803–1812. https://doi.org/10.1261/rna.

79. Signer, R.A.J., Magee, J.A., Salic, A., and Morrison, S.J. (2014). Haematopoietic stem cells require a highly regulated protein synthesis rate. Nature *509*, 49–54. https://doi.org/10.1038/nature13035.

80. Trinh, D.A., Shirakawa, R., Kimura, T., Sakata, N., Goto, K., and Horiuchi, H. (2019). Inhibitor of Growth 4 (ING4) is a positive regulator of rRNA synthesis. Sci. Rep. *9*, 17235. https://doi.org/10.1038/s41598-019-53767-1.

## STAR★METHODS

### KEY RESOURCES TABLE

| REAGENT or RESOURCE | SOURCE | IDENTIFIER |
|---|---|---|
| Antibodies | | |
| TER-119 Monoclonal Antibody (TER119), PE | Invitrogen | Cat#MA5-17824; RRID: AB_2539208 |
| CD3e Monoclonal Antibody (145-2C11), PE | Invitrogen | Cat#12-0031-82; RRID: AB_465496 |
| Ly-6G/Ly-6C Monoclonal Antibody (RB6-8C5), PE | Invitrogen | Cat#12-5931-82; RRID: AB_466045 |
| CD11b/c Monoclonal Antibody (OX42), PE | Invitrogen | Cat#12-0110-82; RRID: AB_11150971 |
| CD45R (B220) Monoclonal Antibody (HIS24), PE | Invitrogen | Cat#12-0460-82; RRID: AB_465692 |
| CD48 Monoclonal Antibody (HM48-1), PE | Invitrogen | Cat#12-0481-82; RRID: AB_465694 |
| CD34 Monoclonal Antibody (RAM34), FITC | Invitrogen | Cat#11-0341-82; RRID: AB_465021 |
| Ki-67 Monoclonal Antibody (SolA15), PE-Cyanine7 | Invitrogen | Cat#14-5698-82; RRID: AB_10854564 |
| PE/Cyanine7 anti-mouse CD150 (SLAM) Antibody | BioLegend | Cat#115913; RRID: AB_2900547 |
| APC/Fire™ 750 anti-mouse CD150 (SLAM) Antibody | BioLegend | Cat#115939; RRID: AB_2629586 |
| Brilliant Violet 510™ anti-mouse Ly-6A/E (Sca-1) Antibody | BioLegend | Cat#108129; RRID: AB_2561593 |
| APC anti-mouse Ly-6A/E (Sca-1) Antibody | BioLegend | Cat#108111; RRID: AB_313348 |
| APC/Cyanine7 anti-mouse CD117 (c-kit) Antibody | BioLegend | Cat#135135; RRID: AB_2632808; RRID: AB_2632808 |
| CD3e Monoclonal Antibody (145-2C11), APC, eBioscience™ | Invitrogen | Cat#17-0031-82; RRID: AB_469315 |
| CD45R (B220) Monoclonal Antibody (RA3-6B2), eFluor™ 450, eBioscience™ | Invitrogen | Cat#48-0452-82; RRID: AB_1548761 |
| Brilliant Violet 510™ anti-mouse/human CD11b Antibody | Invitrogen | Cat#101245; RRID: AB_2561390 |
| APC/Cyanine7 anti-mouse TER-119/Erythroid Cells Antibody | BioLegend | Cat#116223;RRID: AB_2137788 |
| Ly-6G/Ly-6C Monoclonal Antibody (RB6-8C5), PE-Cyanine7, eBioscience™ | Invitrogen | Cat#25-5931-82; RRID: AB_469663 |
| CD45.1 Monoclonal Antibody (A20), PE, eBioscience™ | Invitrogen | Cat#12-0453-82; RRID: AB_465675 |
| CD45.2 Monoclonal Antibody (104), Alexa Fluor™ 700, eBioscience™ | Invitrogen | Cat#56-0454-82; RRID: AB_657752 |
| CD34 Monoclonal Antibody (RAM34), Alexa Fluor 700 | Invitrogen | Cat#56-0341-82; RRID: AB_493998 |
| Chemicals, peptides, and recombinant proteins | | |
| H2DCFDA (H2-DCF, DCF) | Invitrogen | Cat#D399 |
| Bovine Serum Albumin (BSA) | Invitrogen | Cat#B14 |
| Fetal Bovine Serum, qualified, United States | Invitrogen | Cat#26140079 |
| PBS, pH 7.4 | Invitrogen | Cat#100100002 |
| Red Blood Cell Lysis Solution (10x) | Miltenyi Biotec | Cat#130-094-183 |
| Hematoopoietic LIneage Labeling Cockatin, anti-mouse, Biotin | Miltenyi Biotec | Cat#130-092-613 |
| LS Columns | Miltenyi Biotec | Cat#130-042-401 |
| eBioscience™ Intracellular Fixation & Permeabilization Buffer Set | Invitrogen | Cat#88-8824-00 |
| Buffer RLT Plus | Qiagen | Cat#1053393 |
| RNeasy Plus Kits for RNA Isolation | Qiagen | Cat#74034 |
| SYBR™ Green PCR Master Mix | Thermofisher | Cat#4309155 |

(*Continued on next page*)

*Continued*

| REAGENT or RESOURCE | SOURCE | IDENTIFIER |
|---|---|---|
| CellTrace™ Violet Cell Proliferation Kit, for flow cytometry | Thermofisher | Cat#C34571 |
| StemPro™-34 SFM (1X) | Thermofisher | Cat#10639011 |
| Mouse SCF Recombinant Protein, PeproTech® | Thermofisher | Cat#250-03-1MG |
| Mouse TPO (Thrombopoietin) Recombinant Protein, PeproTech® | Thermofisher | Cat#315-14-1MG |
| 5-Fluorouracil, 99% | Thermofisher | Cat#228440250 |
| 10058-F4, Thermo Scientific Chemicals | Thermofisher | Cat#J65650.MA |
| Annexin V Recombinant Protein, APC, eBioscience™ | Thermofisher | Cat#BMS306APC-100 |
| DAPI Solution | Thermofisher | Cat#62248 |
| CellEvent™ Senescence Green Detection Kit | Thermofisher | Cat#C10851 |
| LIVE/DEAD™ Fixable Red Dead Cell Stain Kit, for 488 nm excitation | Thermofisher | Cat#L34971 |
| NEBNext® Single Cell/Low Input cDNA Synthesis & Amplification Kit | New England Biolabs | Cat#E6421S |
| MitoProbe™ TMRM Assay Kit for Flow Cytometry | Thermofisher | M20036 |
| **Deposited data** | | |
| RNA-sequencing | NCBI | https://www.ncbi.nlm.nih.gov/bioproject/1130539 |
| **Experimental models: Organisms/strains** | | |
| Mouse: C57BL/6 (CD45.2) | The Jackson Laboratory | Cat#000664 |
| Mouse: SJL-Ptprc$^{a}$ Pepc$^{b}$/BoyJ (CD45.1) | The Jackson Laboratory | Cat#002014 |
| Mouse: Ing4$^{-/-}$ (CD45.2) | Stephen N. Jones | N/A |
| **Oligonucleotides** | | |
| Actin-Forward | CATCCGTAAAGACCTCTATGCCAAC | N/A |
| Actin-Reverse | ATGGAGCCACCGATCCACA | N/A |
| Gapdh-Forward | ATGTGTCCGTCGTGGATCTGAC | N/A |
| Gapdh-Reverse | AGACAACCTGGTCCTCAGTGTAG | N/A |
| mSrm-Forward | ACATCCTCGTCTTCCGCAGTA | N/A |
| mSrm-Reverse | GGCAGGTTGGCGATCATCT | N/A |
| mRps5-Forward | TGGCAGAGACCCCTGACAT | N/A |
| mRps5-Reverse | GGGCAGGTACTTGGCATACT | N/A |
| mRps3-Forward | ATGGCGGTGCAGATTTCCAA | N/A |
| mRps3-Reverse | GTAACTCGGACTTCAACTCCAG | N/A |
| mRpl34-Forward | TCCAGCGTTTGACATACCGC | N/A |
| mRpl34-Reverse | TAGGTGCTTTCCCAACCTTCT | N/A |
| mNdufb5-Forward | CAGGCTGGACTCAGCTACATC | N/A |
| mNdufb5-Reverse | AGTCTTCATGGCGTTTGCTT | N/A |
| mNdufb4-Forward | CGCTTGGCACTGTTTAATCCA | N/A |
| mNdufb4-Reverse | TCCATGGCTCTGGGTTGTTC | N/A |
| mAtp5me-Forward | GTTCAGGTCTCTCCACTCATCA | N/A |
| mAtp5me-Reverse | CGGGGTTTTAGGTAACTGTAGC | N/A |
| mCited2-Forward | TGCCGCCCAATGTCATAGACAC | N/A |
| mCited2-Reverse | AGAGTTCGGGCAGCTCCTTGAT | N/A |
| mCavin3-Forward | AAGCTGCACGTCCTGCTCTTCA | N/A |
| mCavin3-Reverse | CCAACTTCATCCTCTGGCTGATC | N/A |

(*Continued on next page*)

*Continued*

| REAGENT or RESOURCE | SOURCE | IDENTIFIER |
|---|---|---|
| mHAT1-Forward | GATGGAGCTACGCTCTTTGCGA | N/A |
| mHAT1-Reverse | GCCCTGACCTTGAAATGGAGTC | N/A |
| mActr3-Forward | CAGGCTGAAGTTAAGCGAGGAG | N/A |
| mActr3-Reverse | CCTCCAAACCAGACTGCATACC | N/A |
| mRgs1-Forward | AATGCAGTGGTCTCAGTCTCTGG | N/A |
| mRgs1-Reverse | ATAGTCCTCACAAGCCAACCAGA | N/A |
| mGpx1-Forward | CGCTCTTTACCTTCCTGCGGAA | N/A |
| mGpx1-Reverse | CGCTCTTTACCTTCCTGCGGAA | N/A |
| mTxn1-Forward | CAAATGCATGCCGACCTTCCAG | N/A |
| mTxn1-Reverse | GCTGGTTACACTTTTCAGAGCATG | N/A |
| Software and algorithms | | |
| FlowJo v10.9 | FlowJo™ | N/A |
| GraphPad Prism 10 | Dotmatics | N/A |
| Biorender | Biorender | N/A |

## RESOURCE AVAILABILITY

### Lead contact

Further information and requests for resources and reagents should be directed to and will be fulfilled by the lead contact, Dr. Katie Kathrein (klk@sc.edu).

### Materials availability

This study did not generate any plasmids.

This study did not generate any new mouse lines.

This study did not generate new, unique reagents.

### Data and code availability

RNA-seq data are publicly accessible through NCBI using accession number PRJNA1130539.

This paper does not report original code.

Any additional information required to reanalyze the data reported in this paper is available from the lead contact upon request.

## EXPERIMENTAL MODEL AND STUDY PARTICIPANT DETAILS

### Mice

All mice were bred and maintained at an AALAC-accredited animal facility at the University of South Carolina. Animal experiments were performed according to Institutional Animal Care and Use Committee animal guidelines, and all animal experiments were performed with consent from the local ethical committee. Both female and male mice were used in experiments. Mice of 8–12 weeks of age were used for analysis unless otherwise specified in the text.

Ing4$^{-/-}$ mice (CD45.2) were provided by Stephen N. Jones (University of Massachusetts Medical School) and colony was maintained on site. Wildtype (WT) C57BL/6 (CD45.2) and SJL-Ptprc$^{a}$ Pepc$^{b}$/BoyJ (CD45.1) served as controls. CD45.1 mice were purchased from The Jackson Laboratory.

## METHOD DETAILS

### Bone marrow and peripheral blood preparation

For HSC isolation (Lin$^{-}$Sca$^{+}$c-Kit$^{+}$[LSK]CD48$^{-}$CD150$^{+}$ cell fraction), WBM cells isolated by crushing long bones from each mouse then filtered through a 40μm nylon cell strainer. Cells were incubated with 1x RBC Lysis Solution (Miltenyi Biotec) to lyse red blood cells. Cells were lineage depleted using a Lineage Cell Depletion Kit (Miltenyi Biotec) using LS columns and an LS magnetic separator. Under anesthesia, peripheral blood was collected from retroorbital venous sinus into heparinized (0.05 IU/mL; Alfa Aesar) micro-hematocrit capillary tubes (Kimble). Cells were incubated with 1x RBC Lysis Solution (Miltenyi Biotec) to lyse red blood cells. All experiments have been repeated at least twice unless otherwise noted.

### Flow cytometry

After lineage depletion, WBM cells were incubated for in the dark for 30 min at 4°C with antibodies for HSC profiling (Lineage: B220, CD3e, CD11b, Gr-1, Ter119; Sca-1, c-Kit, CD48, CD34, CD150). Markers used for progenitor cells also included CD16/32 and CD127. For mature blood cells, markers were CD3e, CD45R, Ter119, Ly-6G/C, and CD11b. Following antibody staining, cells were rinsed twice with phosphate-buffered saline (PBS)-bovine serum albumin (BSA). Antibodies against CD45.2 and CD45.1 were used to assess engraftment following transplantation assays. See STAR methods for complete list of antibody sources.

Cells were analyzed on BD LSR II, FACSAria II, or FACSymphony (BD). For sorted cell assays, FACSAria II was used. FACS Diva was used in conjunction with flow cytometers for acquisition and FlowJo (version 10) was used for analysis of HSC populations.

### Cell cycle analysis

Lineage-depleted, stained WBM cells were fixed and permeabilized with Cytofix/Cytoperm kit (Invitrogen) according to manufacturer's instructions. Cells were incubated in the dark overnight at 4°C with Ki67 antibody (Invitrogen), then rinsed with PBS. Prior to analysis via flow cytometry, cells were incubated for 15 min at room temperature with DAPI (0.2 μL/mL, Invitrogen) and rinsed with PBS.

### Reactive oxygen species analysis

Lineage-depleted WBM cells were stained for HSC profiling WBM, then incubated with 7.5μM $H_2$DCFDA (Invitrogen) in PBS for 30 min at 37°C. Cells were rinsed with PBS.

### Senescence assay

Lineage-depleted, stained WBM cells were fixed and permeabilized with Cytofix/Cytoperm kit (Invitrogen) according to manufacturer's instructions. Fixed and permeabilized cells were incubated with CellEvent Senescence Probe (Thermo) for 2 h at 37°C. Cells were rinsed with PBS.

### RNA-seq analysis

Bone marrow from 8 to 10 mice was harvested and pooled, and lineage depleted. LT- and ST-HSCs were sorted separately into Buffer RLT Plus (Qiagen) for both WT or Ing4$^{-/-}$ mice. Total RNA was isolated with the RNeasy Micro column (QIAGEN). Library construction, sequencing by Illumina HiSeq, and initial bioinformatics analyses were conducted by GENEWIZ. Counts obtained were used to perform Gene Set Enrichment Analysis. Ing4$^{-/-}$ LT- and ST-HSCs were compared together against WT LT- and ST-HSCs.

### Quantitative real-time PCR

Bone marrow from 8 to 10 mice was harvested, pooled, and lineage depleted. LT- and ST-HSCs were sorted together into Buffer RLT Plus (Qiagen) for both WT or Ing4$^{-/-}$ mice. Total RNA was isolated with the RNeasy Micro column (QIAGEN). Lineage depleted LT- and ST-HSCs from pools of 8–10 WT or Ing4$^{-/-}$ mice were sorted into Buffer RLT Plus. Total RNA from WT and Ing4$^{-/-}$ mice was extracted with RNA Isolation kit system (QIAGEN) and purified with RNeasy system (QIAGEN). cDNA was prepared with Single Cell/Low Input cDNA Synthesis & Amplification System for RT-PCR (NEB) using oligo-dT primers associated RNA-seq data. (Primer sequences shown in STAR methods) qRT-PCR was performed using the SYBR Green PCR Master Mix (Applied Biosystems). Gene expression changes were quantified as linear ratio to Gapdh.

### Transplantation assays

For competitive WBM transplantation assays, 1 × $10^5$ total lineage-depleted WBM cells were isolated from Ing4$^{-/-}$ donor mice (on CD45.2 background) or WT donor mice (on CD45.2 background). An additional 4 × $10^5$ lineage-depleted WBM marrow cells were isolated from WT mice (on CD45.1 background) as competitor cells. Donor (CD45.2) and competitor (CD45.1) cells were transplanted via retroorbital injection into 8- to 12-week-old recipient mice (B6. SJL-CD45.1) that had been lethally irradiated (9.5 Gy, administered as two doses at least 3 h apart). Peripheral blood of recipient mice was analyzed at 4 and 12 weeks post-transplant.

For competitive transplantation assays, 10 LT-HSCs or 50 ST-HSCs isolated from Ing4$^{-/-}$ or WT donors (CD45.2) were combined with 200,000 CD45.1 total, unfractionated WBM cells and transplanted into lethally irradiated recipient mice (CD45.1). Flow cytometry analysis was performed using a BD LSRII and sorting was performed using a BD FACSAria II cytometer. Data was analyzed using FlowJo version 10.6.2 software. Antibodies used are provided in the STAR methods.

### Cell proliferation assay

Lineage-depleted WBM cells were stained with 5μM CellTrace Violet (ThermoFisher Scientific) for 20 min at 37°C. Cells were then incubated in complete culture medium for 5 min at 37°C to absorb unbound dye. Washed cells were incubated in STEMPRO medium (Gibco) supplemented with SCF (10 ng/mL, Peprotech) and TPO (100 ng/mL, Peprotech) for 7 days and analyzed by flow cytometry for HSC panel.

### 5-Fluorouracil treatment

Under anesthesia, 8- to 12-week-old Ing4$^{-/-}$ and WT mice received one retroorbital venous sinus injection of 5-fluorouracil (5-FU, 150 mg/kg, Sigma) or PBS. WBM was harvested 15 or 30 days following 5-FU or mock treatment, lineage depleted, stained using HSC panel, and analyzed via flow cytometry.

### c-Myc inhibition

Mice were subjected to 3.5 Gy total body irradiation (Rad Source). c-Myc inhibitor 10058-F4 was dissolved in a mixture of ethanol, Kolliphor, and saline (1:1:8 v/v/v) to a final concentration of 2 mg/mL. Sublethally irradiated (3.5 Gy) 8- to 12-week-old Ing4$^{-/-}$ and WT mice were treated (retroorbital injection) with 20 mg/kg of 10058-F4 or vehicle (ethanol, Kolliphor, saline only) once per day for 14 days. On day 15, bone marrow was analyzed via flow cytometry.

## QUANTIFICATION AND STATISTICAL ANALYSIS

Mean values ±SD are shown. Student's t test with Welch's correction was used for single comparisons (GraphPad Prism v.10.1.1). *$p < 0.05$, **$p < 0.01$, ***$p < 0.005$, ****$p < 0.001$. Two-way ANOVA was used for multiple comparisons for *in vivo* inhibitor assays (GraphPad Prism v.10.1.1). Mann-Whitney test was used to determine chimerism post-WBM transplant.